LEVEL II

(12)

AD-TR- 80-74

FINAL REPORT

AD A096530

DESIGN AND ANALYSIS
OF A
SEISMICALLY STABLE PLATFORM

BY DR. MARTIN G. JAENKE

CONDUCTED FOR

CENTRAL INERTIAL GUIDANCE TEST FACILITY

6585TH TEST GROUP

HOLLOMAN AIR FORCE BASE, NEW MEXICO

AUGUST 1980

Approved for public release; distribution unlimited.

ARMAMENT DIVISION

AIR FORCE SYSTEMS COMMAND • UNITED STATES AIR FORCE

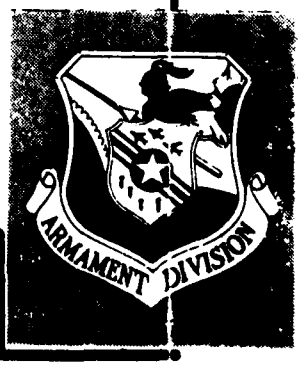

81 2 2 072

THIS TECHNICAL REPORT HAS BEEN REVIEWED AND IS APPROVED:

Robert E. Beale

ROBERT E. BEALE, Colonel, USAF
Deputy Commander

UNCLASSIFIED

SECURITY CLASSIFICATION OF THIS PAGE (When Data Entered)

REPORT DOCUMENTATION PAGE		READ INSTRUCTIONS BEFORE COMPLETING FORM
1. REPORT NUMBER 14 AD-TR-80-74	2. GOVT ACCESSION NO. AD-A096 530	3. RECIPIENT'S CATALOG NUMBER
4. TITLE (and Subtitle) (6) DESIGN AND ANALYSIS OF A SEISMICALLY STABLE PLATFORM, AN EVALUATION		5. TYPE OF REPORT & PERIOD COVERED 9 FINAL REPORT,
		6. PERFORMING ORG. REPORT NUMBER
7. AUTHOR(s) (10) Dr. Martin G. Jaenke		8. CONTRACT OR GRANT NUMBER(s)
9. PERFORMING ORGANIZATION NAME AND ADDRESS 6585th Test Group/GD Holloman AFB, NM 88330		10. PROGRAM ELEMENT, PROJECT, TASK AREA & WORK UNIT NUMBERS JON: (16) 995(4)NO36 (17) NO
11. CONTROLLING OFFICE NAME AND ADDRESS (11)		12. REPORT DATE August 1980
		13. NUMBER OF PAGES 50 (12) 55
14. MONITORING AGENCY NAME & ADDRESS (if different from Controlling Office)		15. SECURITY CLASS. (of this report) UNCLASSIFIED
		15a. DECLASSIFICATION DOWNGRADING SCHEDULE

16. DISTRIBUTION STATEMENT (of this Report)

Approved for public release; distribution unlimited.

17. DISTRIBUTION STATEMENT (of the abstract entered in Block 20, if different from Report)

18. SUPPLEMENTARY NOTES

19. KEY WORDS (Continue on reverse side if necessary and identify by block number)

Seismology	Gyroscopes
Seismic Detection	Transfer Functions
Accelerometers	Seismometers

20. ABSTRACT (Continue on reverse side if necessary and identify by block number)

This paper analyzes a Technical Report (TR 7015.003) furnished to the 6585th Test Group by Measurement Analysis Corporation, in support of the Seismically Stable Platform project. There are six major conclusions.

1. The proposed passive system is basically sound. An active system should improve transmissibility over the estimates given in the MAC report.

DD FORM 1 JAN 73 1473

UNCLASSIFIED 395 046

SECURITY CLASSIFICATION OF THIS PAGE (When Data Entered)

Block 20 (Cont'd)

2. Platform rocking modes may be induced by purely translational ground motion.

3. Apparent platform rocking would be seen by mismatched seismometer pairs. It is not clear that seismometers can be matched to monitor small rotations.

4. The 6585th Test Group should further characterize the rotational and translational motions of the test site.

5. In the future, test analysts should be able to separate test item errors from platform-induced motions. By monitoring known events such as airplane overflights and sled runs, the analyst can account for much of the induced vibration.

6. By band-selectable analysis, the analyst can disregard much of the input vibration. He needs to take into account only those vibrations and rotations that the test item is sensitive to.

Evaluation of

Measurement Analysis Corporation Technical Report # TR 7015.033

dated 25 June 1980

Design and Analysis

of a

Seismically Stable Platform

by: Dr. Martin G. Jaenke

for: 6585th Test Group

7 August 1980

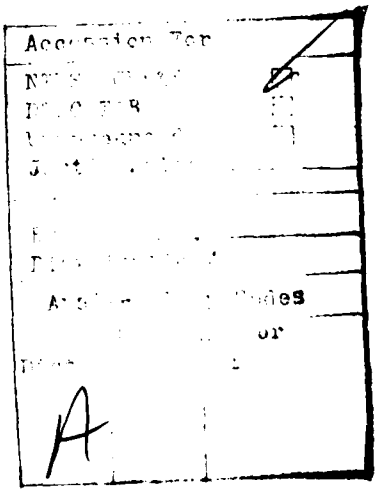

List of Contents:

1. Introduction:

Subject report was prepared by Measurement Analysis Corporation (MAC) under contract for 6585th Test Group. Its principal purpose was the design of a high precision test platform suitable for the testing of future generations of inertial guidance components and systems. This platform also will serve as a prototype facility for test concept verification for a planned Precision Guidance Test Facility.

This evaluation of the report was performed by Dr. Martin G. Jaenke serving as a consultant in a temporary employment limited to 200 hours. The emphasis of the evaluation was on predicting the performance of the proposed system under realistic assumptions of seismic disturbance inputs and on the critical analysis of some design details which are not covered sufficiently in subject report.

Due to the limited time available, all numerical calculations required for the analysis were performed by using manual methods (pocket calculator) because it was felt that the development of new or the adaptation of existing computer programs would be too time consuming. This involved certain simplifications, however, the results obtained provide at least an "order of magnitude" picture of trends.

In the following paragraphs the notation p. XX refers to page XX of subject report. To facilitate typing, all sketches, formulas and tables are comprised on "plates", refered to a Pl YY.

Appendix A contains a short discussion of the possible approaches to present variables which are only statistically defined, a problem which frequently led to confusion.

Appendix B is a copy of a paper which the author presented to the AIAA in 1974. Besides being useful for explaining the assumptions of seismic disturbances made in the evaluation, it is thought to be valuable in the planning process for a future Precision Guidance Test Facility.

2. System Overview:

The system is described in subject report on p. 3 through p. 46. Pl 1 gives a short description sufficient for the understanding of the discussion in the following paragraphs. It shows that the system is a dual isolation system. The primary reaction mass M2 carries the payload PL (test stand and test item) and the instrumentation I necessary to sense the motion of the mass. The secondary reaction mass M1 is a necessary prerequisite to make the dual isolation concept possible. The advantage of this concept is that it provides significantly higher high frequency attenuation of seismic disturbance inputs from the ground than a simple mass-spring system. There are two separate sets of springs, S. The spring action is provided by pneumatic isolators (Barry Serva-Level Pneumatic Isolators #133-12). The vertical (S_V) and horizontal (S_H) spring actions are generated within the same unit. The vertical action is truly pneumatic while the horizontal action is due to the elastic properties of a diaphragm which supports the load carrying element (for detailed description see p. C-8 and p. K-34). Electomagnetic actuators A operate on the primary reaction mass following commands derived from the instrumentation I and processed by appropriate servo loop elements.

The performance of the proposed platform, to the extent that it is relevant for the following discussion, is described in Pl 2 - Pl 4. This performance description is in terms of the transmissibility between the disturbance motion input from the ground and the resulting motions of the primary reaction mass. The information is taken directly from subject report and is accepted at face-value at this point of discussion. A proposed revision of the performance indicators is described in para 3.3 of this evaluation and its consequences for testing performance will be discussed.

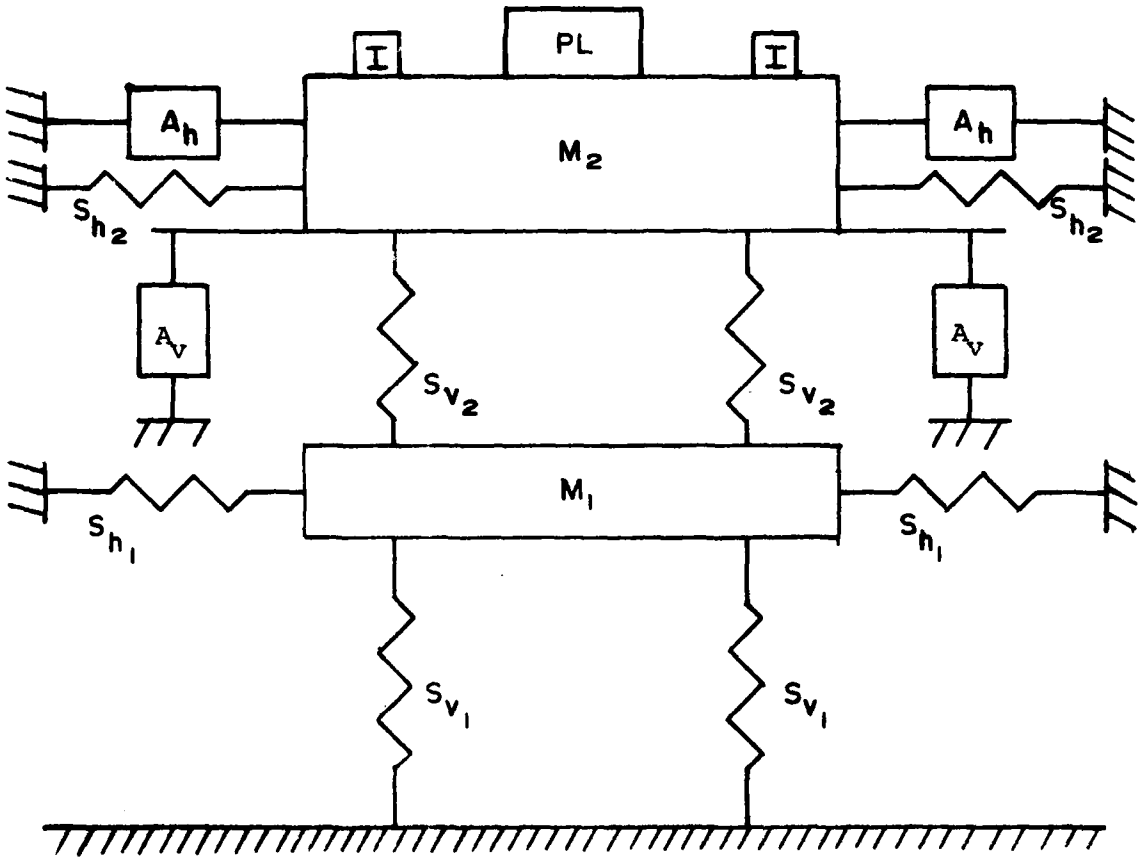

System Concept

Plate 1

HORIZONTAL TRANSMISSIBILITY

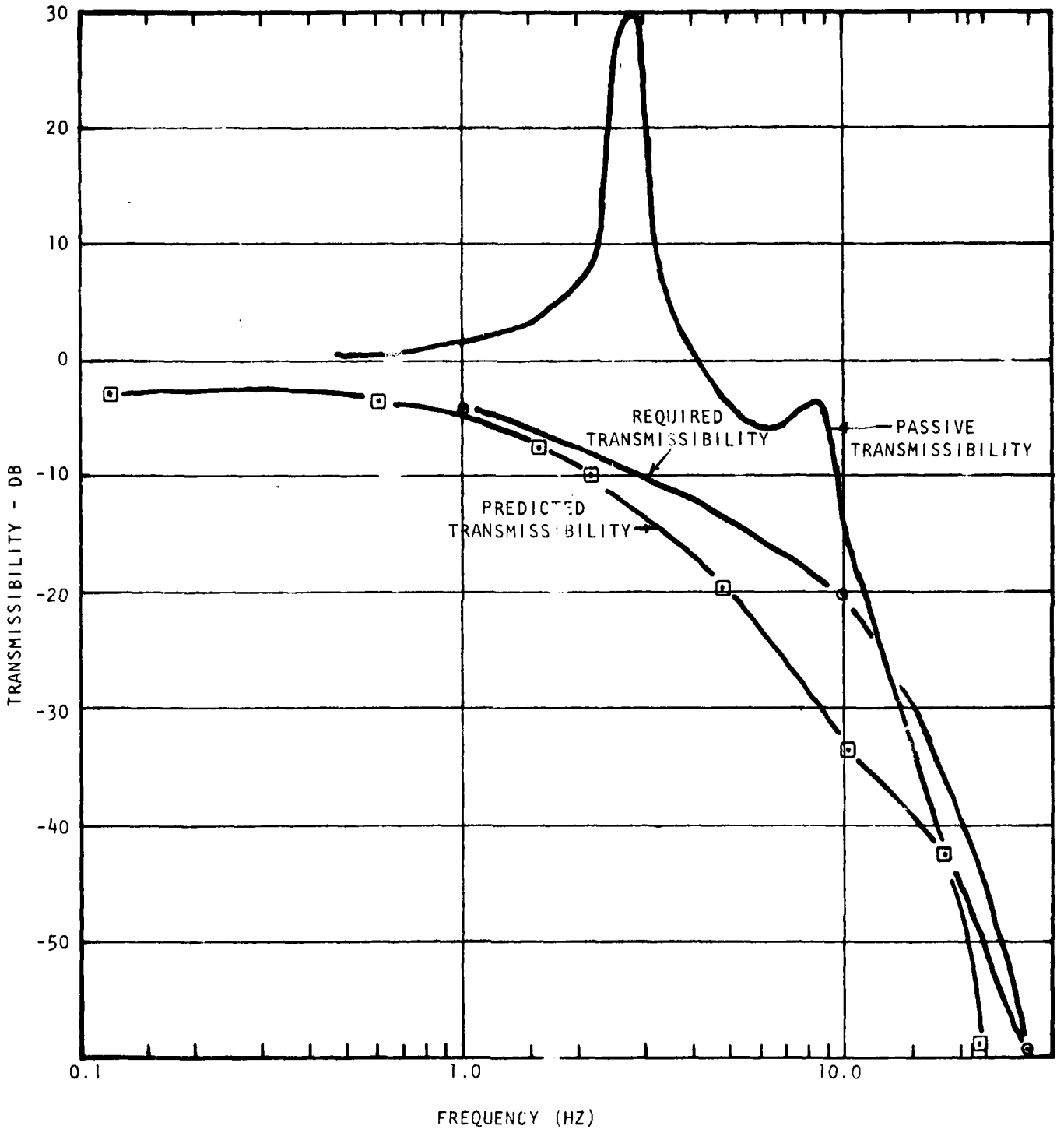

Plate 2

VERTICAL TRANSMISSIBILITY

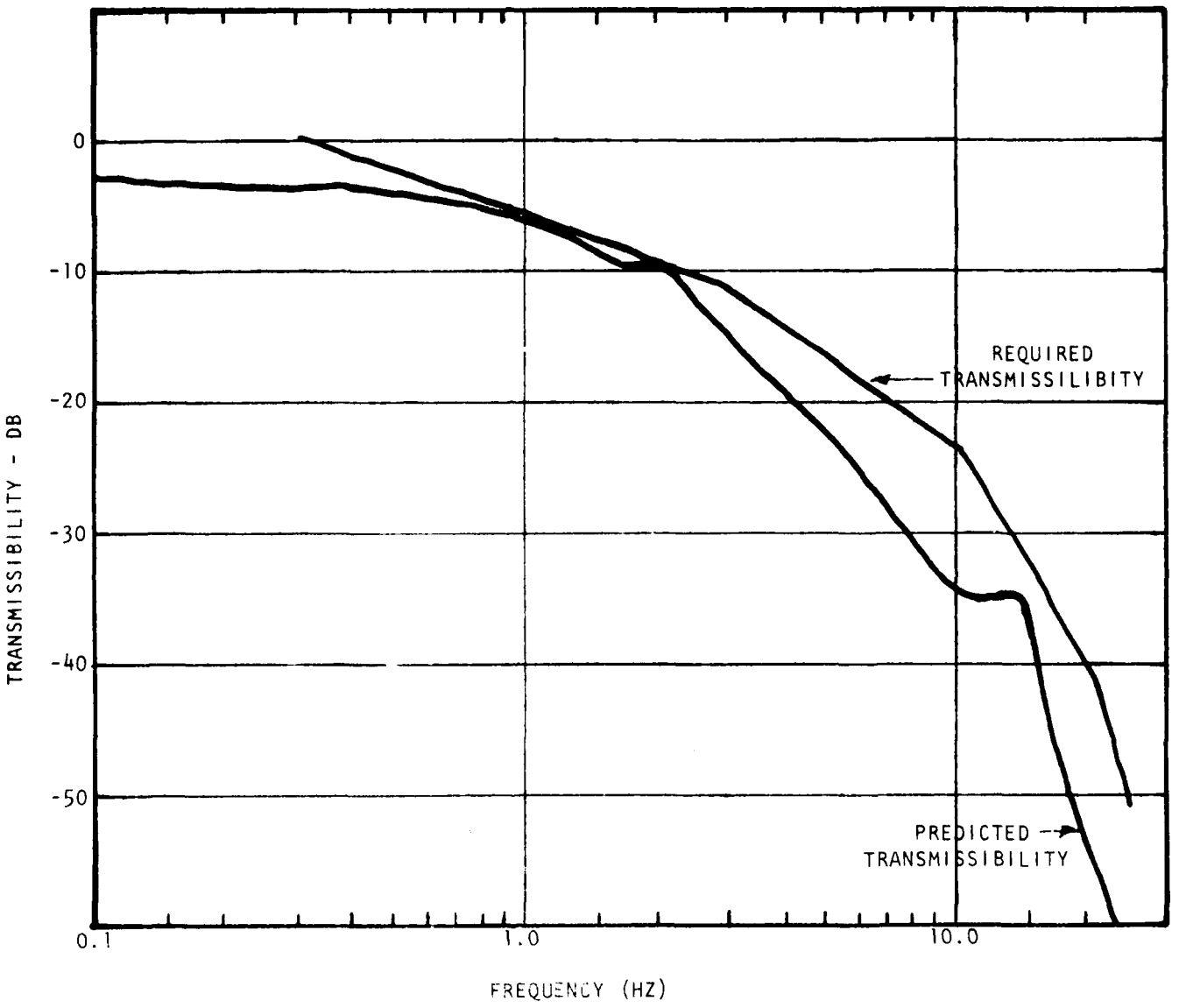

PLATE 3

ACTIVE ANGULAR TRANSMISSIBILITY

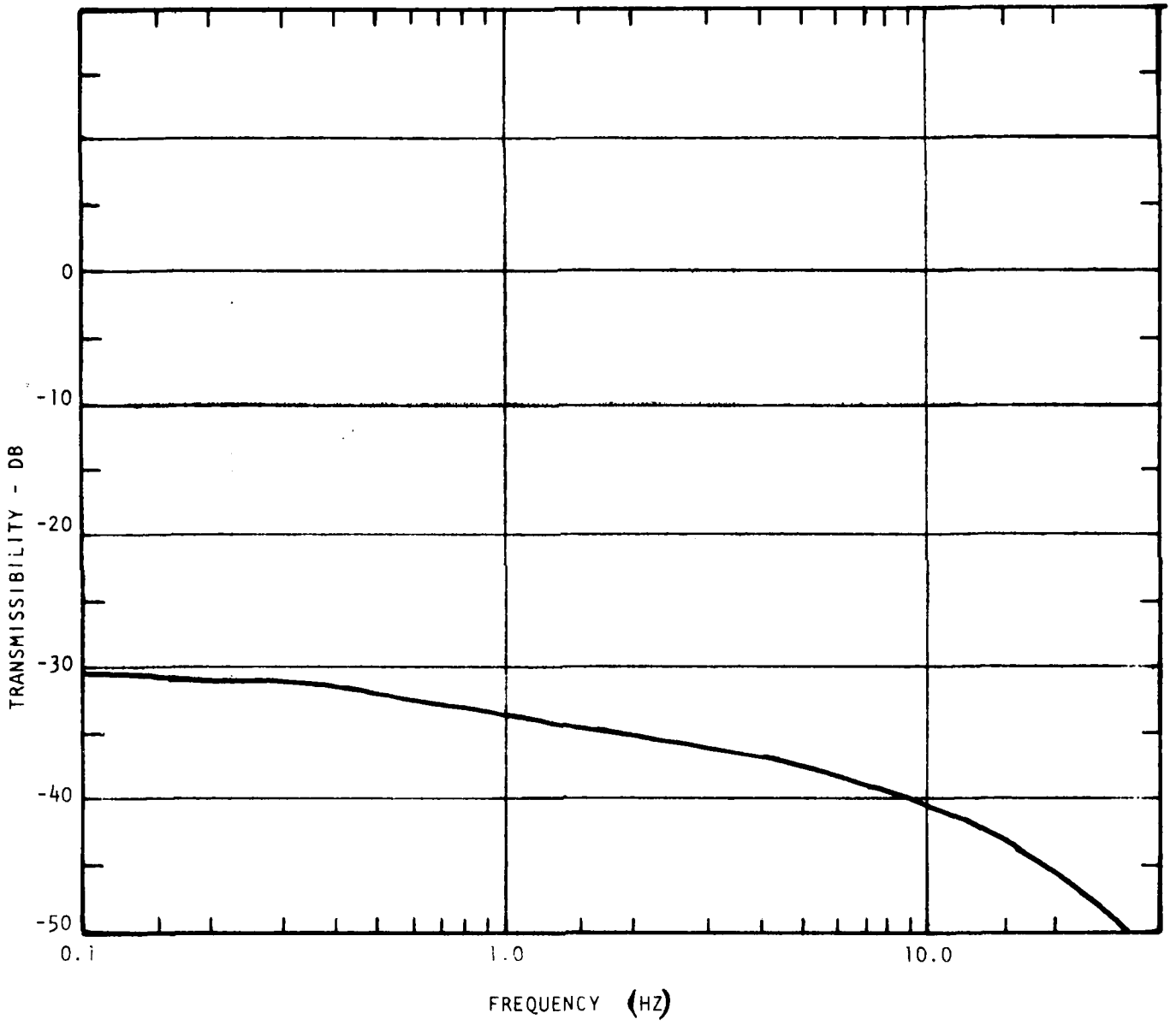

PLATE 4

Pl 2 and 3 describe the transmissibility for translational motions in the horizontal and vertical directions. Pl 2 shows first as a function of frequency the "passive" transmissibility, i.e. the performance of the system with the active control servo loop not in operation. Next, both show the required transmissibility which is necessary to reduce the disturbance inputs which were actually observed in AITL to the specified level of 10^{-8}g. These disturbance inputs agree reasonably well with observations made previously by the author and derived from the literature. Finally, Pl 2 and 3 present the transmissibility predicted with the active stabilization system in operation. It is shown that the system specifications with respect to translational motions are expected to be met, a result which is intuitively accepted by this author. This is not the case with respect to rotational (angular) motions which have significantly more severe consequences on gyro and accelerometer tests than translational disturbances. Unfortunately, the whole area of rotational transmissibility is treated only superfically in subject report and therefore will be the object of a critical analysis in para 3.3 of this evaluation.

Pl 4 presents the expected angular transmissibility from subject report. It will be noted that the plate does not contain information on passive and required transmissibility. The former can not be found anywhere in subject report and the latter deficiency is due to the fact that the contractor did not use information on angular disturbance inputs although it was availabie to him. However, as stated above, Pl 4 will be used at face-value for the following analysis of the effects of angular motions on test accuracy. Pl 5 shows the angular disturbance inputs in terms of a power density spectrum which must be expected for the operation of the proposed platform. It is taken from Fig 5 of Appendix B where detailed information on its conceptional background can be found. The essential features of this spectrum are repeated as curve A in Pl 6, but here in terms of an amplitude spectrum (for a discussion of these different types of presentation see Appendix A). Curve B of Pl 6 shows the resulting platform motions obtained after

ANGULAR GROUND MOTION ENVIRONMENT

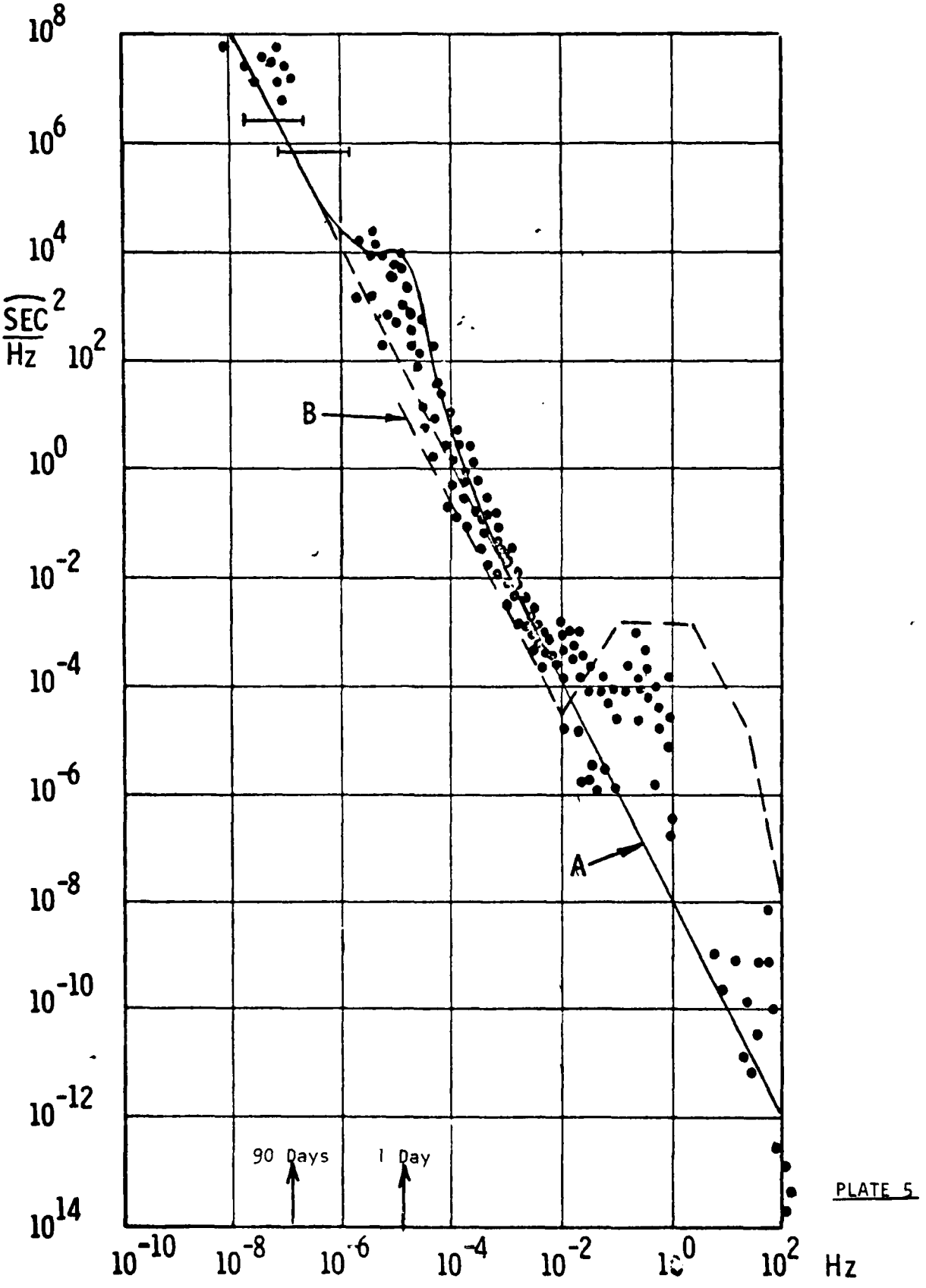

PLATE 5

RMS ANGULAR MOTION ENVIRONMENT

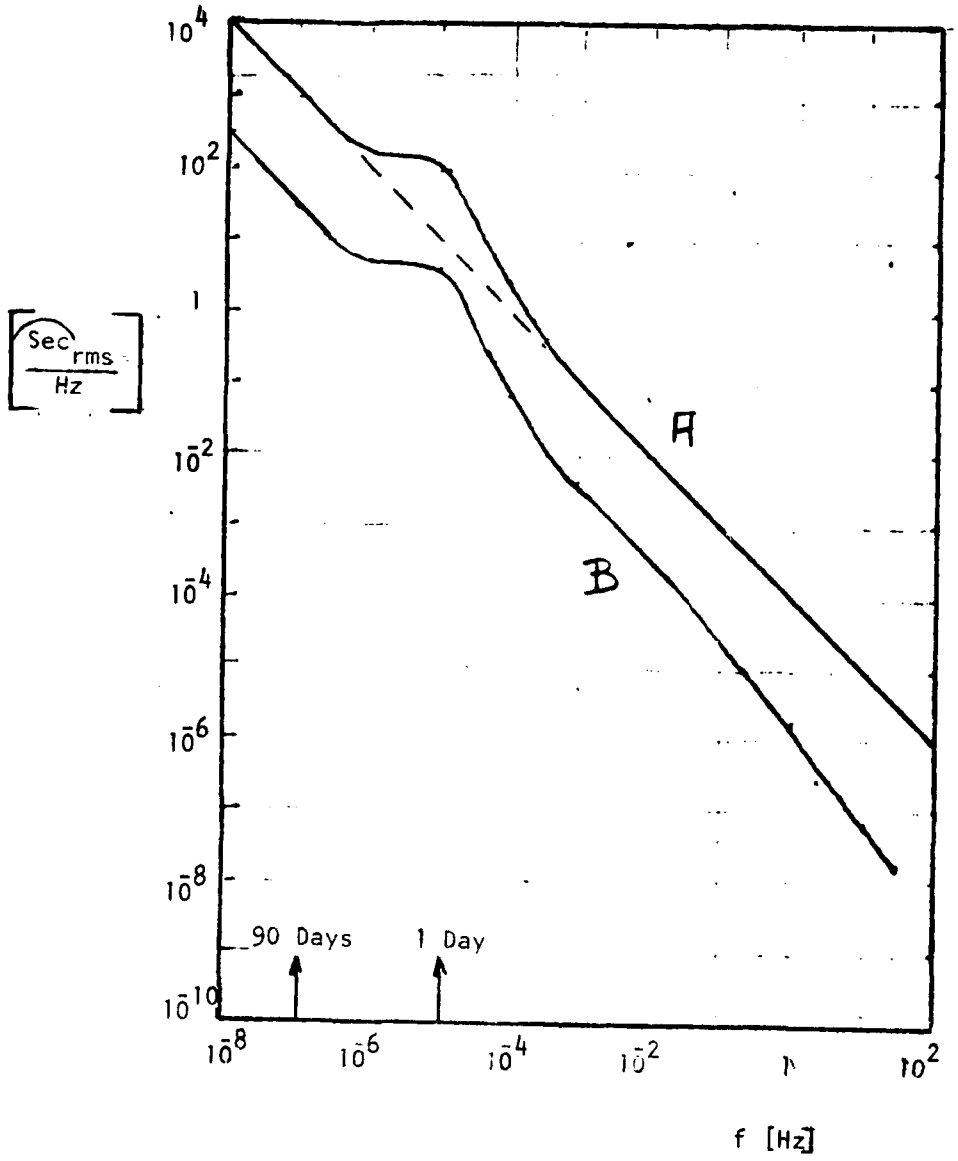

A: ON GROUND

B: ON MAC PLATFORM

PLATE 6

attenuation by the active isolation system in accordance with Pl 4. Pl 7 shows the growth of angular platform deflection with time derived from the spectra of Pl 6, curve A without and curve B with the active isolation system in operation. It is of interest to note that B attains a final value of about 0.02 $\widehat{sec}$, a value which served as a specification for the design contract. Pl 8 shows the spectra of drift induced by platform angular motions into a gyro under test, again without and with platform stabilization. There are two mechanisms causing this drift: one, essentially inversely proportional to frequency at low frequencies is the "pick-up" of components of the earth rotation vector due to angular deflections of the test item. The other, essentially constant at higher frequencies, is due to the sensing of angular rates by the input axis of the gyro under test. The total rms drift value in the frequency band from 10^{-8} to 30 Hz is 4.3×10^{-3} deg/hr without and 5×10^{-5} deg/hr with active isolation. These values are obtained by numerical integration of the power spectra which correspond to the amplitude spectra of Pl 8. It is seen that even with active isolation the platform does not reach a goal of 10^{-6} deg/hr, a goal which was obtained from Pl 9 which is taken from Ref 1.

A similar situation prevails in accelerometer testing. Pl 10 shows the accelerations induced by angular platform deflections which lead to the "pick-up" of components of the gravity vector. The total rms value, obtained in the same way as with Pl 8, while improving from 9×10^{-6} to 3×10^{-7} g_{rms} by using the active isolation, does not reach a goal of 10^{-8} g_{rms} which was obtained from Pl 11, again taken from Ref 1. It is important to note that the acceleration errors induced by angular platform motion can not be reduced to the goal of $10^{-8}g$ while the errors induced by translational platform motions apparently can, as was discussed in connection with Pl 2 and Pl 3 above.

While the proposed platform does not reach the ideal goals formulated in connection with the testing of very advanced future inertial

GROWTH OF PLATFORM ANGULAR UNCERTAINTY WITH TIME

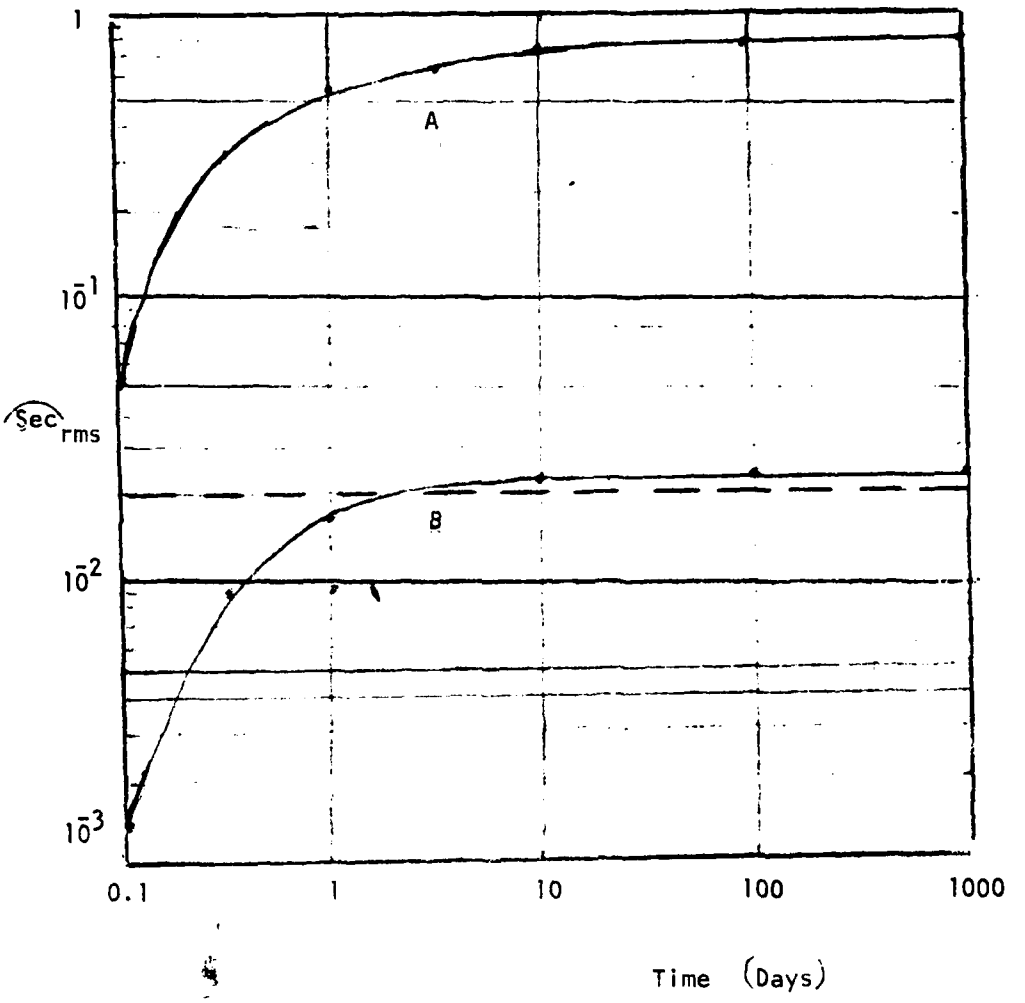

A: PLATFORM ON GROUND

B: MAC PLATFORM

Plate 7

GYRO TESTING

PLATFORM - INDUCED

GYRO DRIFTS

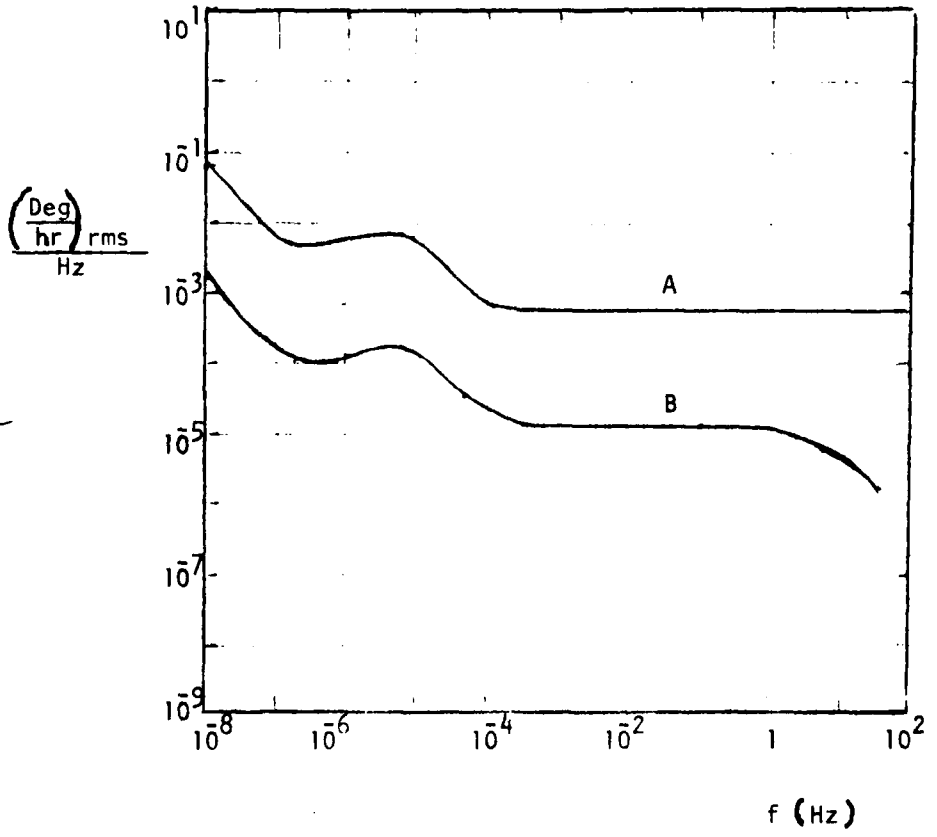

A: PLATFORM ON GROUND

B: MAC PLATFORM

RMS DRIFT IN BAND FROM
10-8 HZ TO 30 HZ

A: 4.3×10^{-3} [DEG/HR] RMS

B: 5×10^{-5} [DEG/HR] RMS

GOAL: 10^{-6} [DEG/HR] RMS

PLATE 8

INERTIAL GRADE
GYROSCOPE ACCURACY
TRENDS

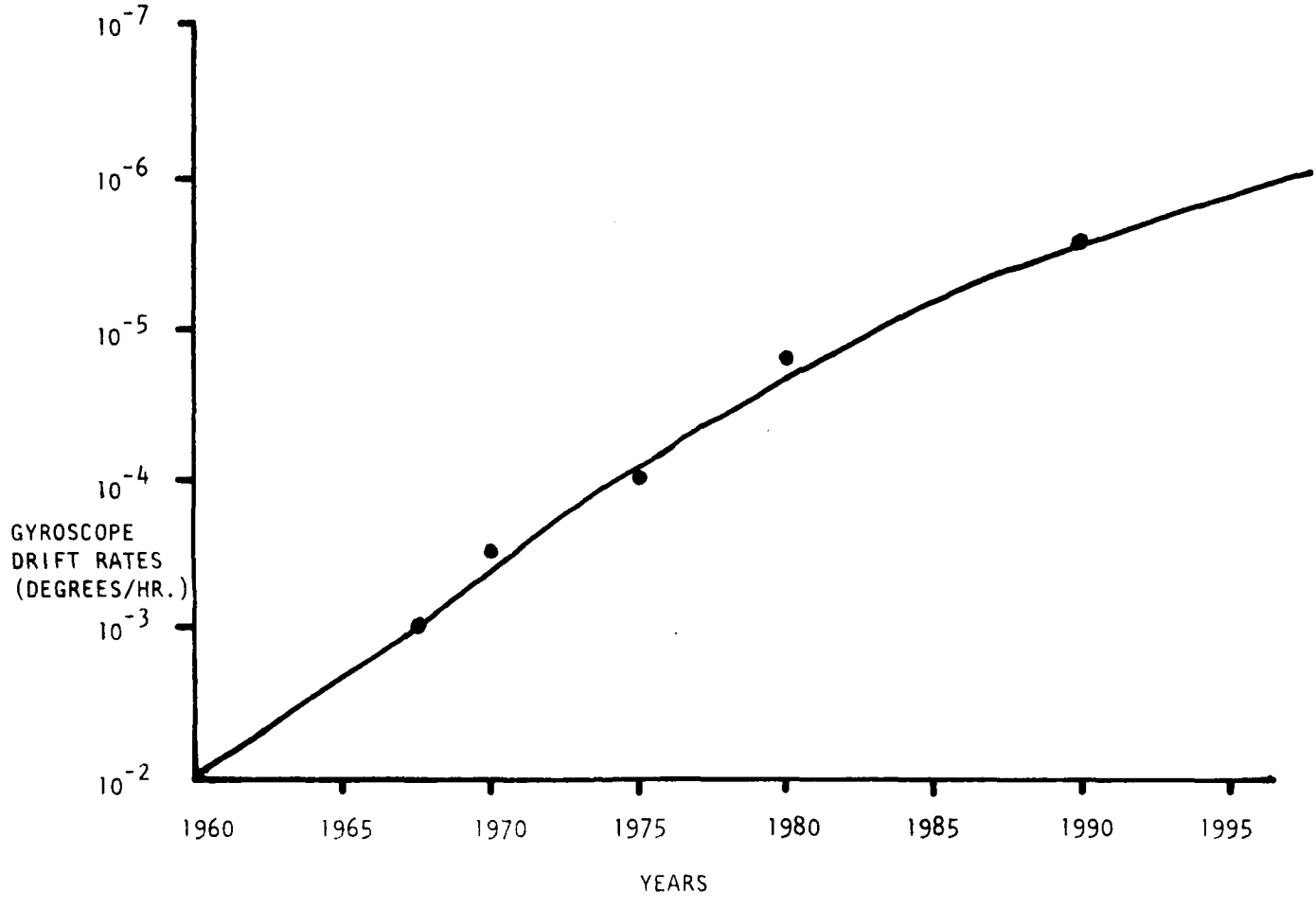

PLATE 9

ACCELEROMETER TESTING

ACCELERATIONS INDUCED BY

ANGULAR PLATFORM MOTIONS

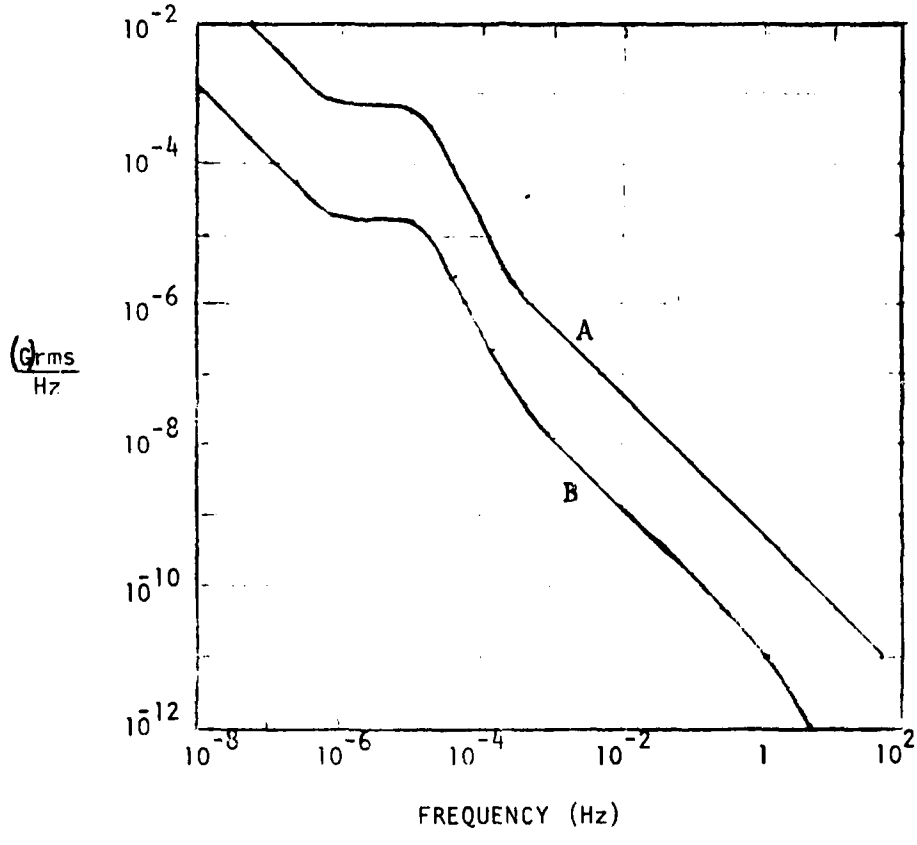

A: PLATFORM ON GROUND

B: MAC PLATFORM

RMS VALUE IN BAND FROM 10^{-8} HZ TO 30 HZ

A: 9×10^{-6} g_{RMS}

B: 3×10^{-7} g_{RMS}

GOAL: 10^{-8} g_{RMS}

PLATE 10

INERTIAL GRADE
ACCELEROMETER ACCURACY
TRENDS

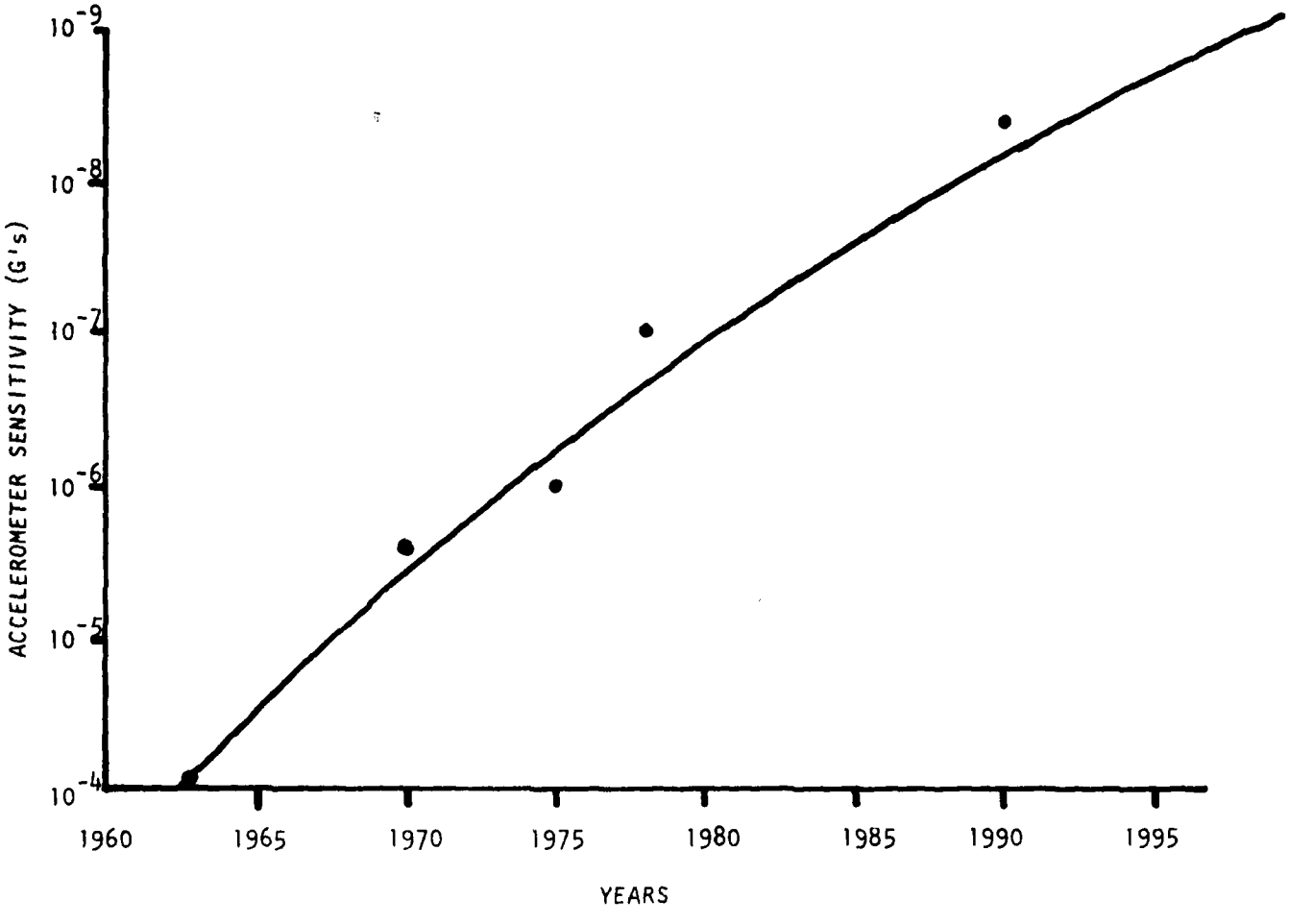

PLATE 11

instruments, it is of interest to compare its performance with that of precision platforms either in existence or under development at other test facilities. Pl 12 provides this comparative information, curve A for the proposed platform (taken from Pl 4) and curve B for the existing platform at the Frank J. Seiler Research Laboratory (information taken from Fig. 6 of Ref. 2 or Fig. 7 of Ref. 3). Curve C presents the results obtained from a prototype precision platform which was developed for the now discontinued NASA Electronic Center in Cambridge, MA. The information is taken from Fig. 31 of Ref. 4. A and B are equal in the high frequency range but B is inferior in the middle range which contributes quite significantly to the overall rms test error value. C is inferior to both except in the low frequency range. Thus, is seems that the proposed system is at least compatible with the apparent state of the art and superior to other systems.

3. Detail Analysis:

3.1 Induced Rocking Motions

The structural lay-out of the proposed platform lends itself to the induction of rocking motions, i.e. the generation of angular motions by translational motions. The sketch on Pl 13 explains the two mechanisms through which these rocking motions are excited. One of these mechanisms, in the following called mechanism C, is due to the translational acceleration, a, operating on the center of gravity (CG) of the primary reaction mass which is displaced by the lever arm z from the neutral plane. In this way a torque is produced which leads to angular motions about CG. The other mechanism, called mechanism B in the following, is due to the difference between the translational displacement of the ground and that of the platform. For the quantitative analysis of these mechanisms a single stage instead of a dual stage isolation

COMPARISON
OF
ACTIVE STABILIZATION SYSTEMS
(ATTENUATION OF ANGULAR GROUND MOTIONS VERSUS FREQUENCY)

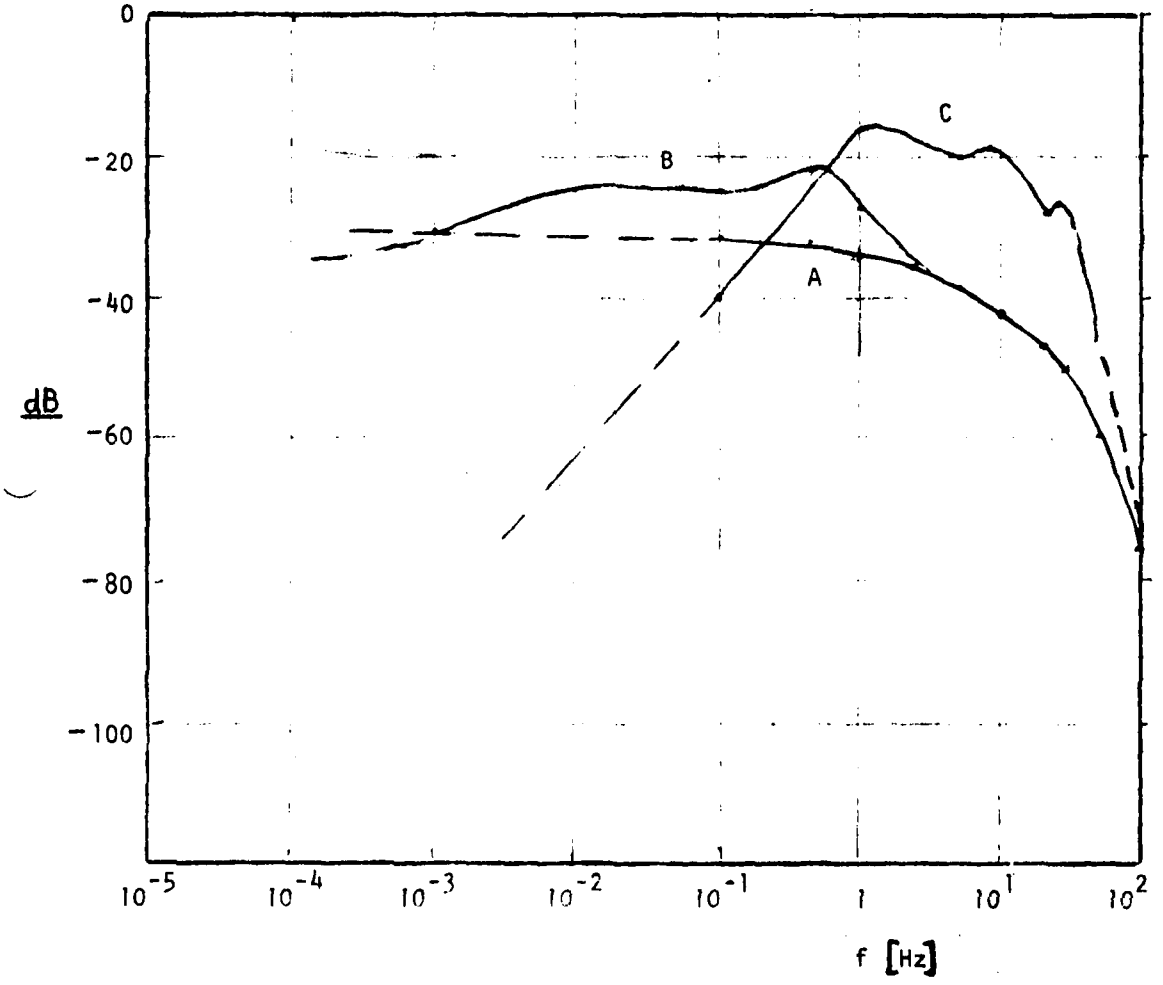

A: MAC

B: FRANK J. SEILER RESEARCH LABORATORY
(BILL J. SIMMONS)

C: EXPERIMENTAL SYSTEM AT THE DISCONTINUED NASA ELECTRONICS CENTER IN CAMBRIDGE, MA (HERBERT WEINSTOCK)

PLATE 12

EXCITATION OF ROCKING MOTIONS

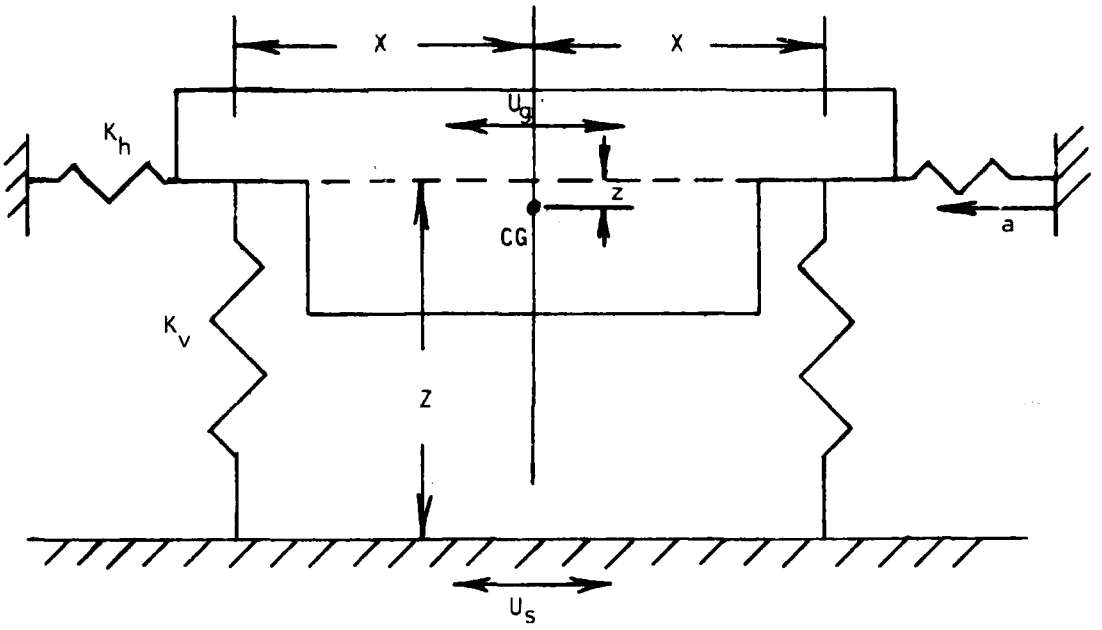

U_s: Lateral ground displacement (in)

U_g: Lateral platform displacement (in)

a: Lateral platform acceleration $(\frac{in}{sec^2})$

X: 53 in
Z: 28 in } from DD 7015.003

z: 2.8 in from p.E-34 (Vol. I)

M_2: Mass of Primary mass; 44.2 $\frac{lb\ sec^2}{in}$ from p.E-33

M_t: Mass of total system; 68.7 $\frac{lb\ sec^2}{in}$ from p. E-106

I_2: Moment of inertia of primary mass; 3.25×10^4 lb sec^2 in

I_t: Moment of inertia of total system; 6.43×10^4 lb sec^2 in

$I = \Sigma m_i d_i^2$; m_i from p. E-102ff
d_i from p. E85ff

K_h: Horizontal spring constant: 1.42×10^4 $\frac{lb}{in}$

K_v: Vertical spring constant: 3.13×10^3 $\frac{lb}{in}$ } calculated from C-55 and C-54 respectively

S_h: Rotational spring constant: 8.8×10^6 lb in about horizontal axis: $S_h = k_v \cdot X^2$

PLATE 13

system was assumed to be able to use transfer functions from the available literature. This simplified analysis is considered adequate to yield order-of-magnitude information on the effects. The pertinent coefficients for this analysis were derived from the transmissibility function on p. C-54 and p. C-55 under the assumption that these functions were generated by a single stage system. The transfer function for mechanism B on Pl 14 is transcribed from equation (5) of Ref. 5. The transfer function for mechanism C is straightforward. The flow chart on Pl 15 shows the steps to be taken to compare the various angular motions while the active angular stabilization loop is not in operation but the horizontal active loop is. Pl 16 is a compilation of all the calculations performed and Pl 17 is a graphical presentation of the results. It is seen that the various motion components are essentially of the same order of magnitude. There is no evidence of a catastrophic excitation of rocking motions. However, the analyst of future gyro and accelerometer test results must be aware that such rocking mechanisms exist, must look out for them in his test data, and, if they are found, must avoid attributing them to the test item.

3.2 Instrumentation Concept

The instrumentation philosophy of subject report is quite interesting. In contrast to other high precision stabilized platforms which use two different types of instruments to be able to measure all platform motions over the frequency range of interest, the report proposes to use only one type. The instruments in question are seismometers, of which 4 will be provided to measure motions in the horizontal and 4 in the vertical plane. The manufacturer of the seismometers is Sprengnether Instruments, Inc., and the type numbers are S-5100-H for the horizontal and S-5100-V for the vertical instruments. The seismometers are of the spring-mass type and the deflection of the proof mass is measured either by a coil (velocity pick-off) or a capacitance

R_h: Horizontal damping force coefficient: $3.17 \times 10^1 \frac{lb}{in}$ sec

R_v: Vertical damping force coefficient: $1.51 \times 10^1 \frac{lb}{in}$ sec } From C-55 and C-54

H_h: Rotational damping force coefficient about horizontal axis:
$H_h = R_v \cdot X^2 = 4.24 \times 10^4$ lb in sec

Rocking Mechanism B

$$\Theta = \frac{(U_s - U_g)\ (SZR_h - Zk_h)}{S^2 I_t + S(H_h + Z^2 R_h) + (S_h + Z^2 K_h)}$$

$$\frac{\Theta}{\Delta U} = \frac{S(28 \times 3.17 \times 10^1) - (28 \times 1.42 \times 10^4)}{S^2(6.43 \times 10^4) + S(4.24 + 10^4 + 7.84 \times 10^{-2} \times 3.17 \times 10^1) + (8.8 \times 10^6 \times 7.84 \times 10^2 \times 1.42 \times 10^4)}$$

$$\frac{\Theta}{\Delta U} = \frac{S(4.47 \times 10^{-5}) - (2 \times 10^{-2})}{S^2(3.23 \times 10^{-3}) + S(3.38 \times 10^{-3}) + 1}$$

Frequency = 2.8 Hz

DC Gain: 2×10^{-2}

Resonance Peak (relative): 16.8

Rocking Mechanism C

$$aM_2 \cdot Z = \Theta[S^2 I_2 + SH_h + S_h]$$

$$\frac{\Theta}{a} = \frac{M_2 Z}{S^2 I_2 + SH_h + S_h} \quad ; \quad \frac{\Theta}{a} = \frac{(44.2 \times 2.8)}{S^2(3.24 + 10^4) + S(4.24 + 10^4) + (8.8 \times 10^6)}$$

$$\frac{\Theta}{a} = \frac{1.4 \times 10^{-5}}{S^2(3.68 \times 10^{-3}) + S(4.82 \times 10^{-3}) + 1}$$

Frequency = 2.62 Hz

DC Gain: 1.4×10^{-5}

Resonance Peak (relative): 12.5

PLATE 14

COMPARISON OF ANGULAR PLATFORM MOTION COMPONENTS

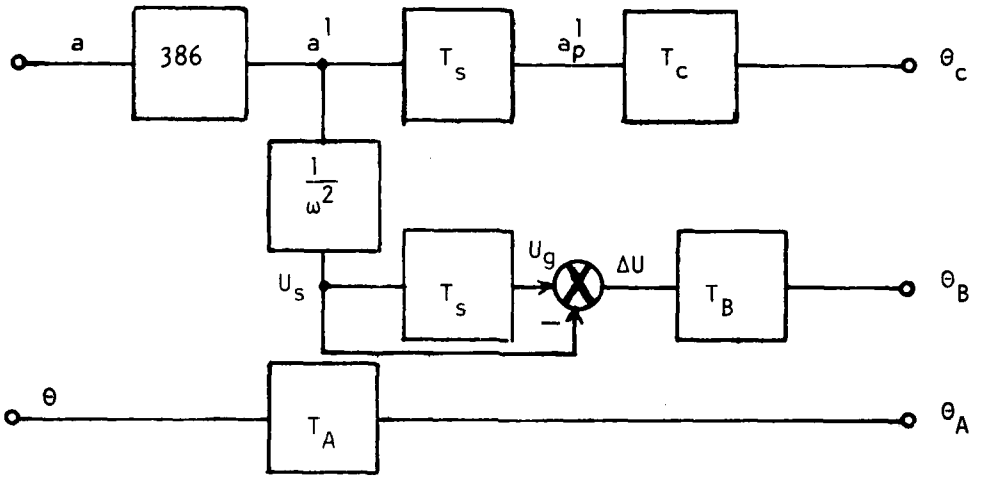

a: Horizontal acceleration input [g]; from p.H-18

a^1: Horizontal acceleration input $[\frac{in}{Sec^2}]$

a_p^1: Horizontal platform acceleration $[\frac{in}{Sec^2}]$

U_s: Horizontal ground displacement [in]

U_g: Horizontal platform displacement [in]

θ: Rotational displacement input [$\widehat{Sec}$]; from PI 6

T_s: Horizontal active transfer function; from PI 2

T_A: Passive angular transfer function; from PI 22

T_C: Transfer function $\frac{\theta}{a}$ } from PI 12

T_B: Transfer function $\frac{\theta}{\Delta U}$

PLATE 15

$f_{[Hz]}$	a [g]	a' [in/Sec^2]	T_s	a'_p	T_c	Θ_c [Sec]	U_s [in]	U_g	ΔU	T_B	Θ_B [Sec]	T_A	Θ_A [Sec]
100	2.5×10^{-6}	9.6×10^{-4}	3.5×10^{-5}	3.4×10^{-8}	9.8×10^{-9}	6.7×10^{-11}	2.4×10^{-9}	8.6×10^{-14}	2.4×10^{-9}	2.8×10^{-5}	1.35×10^{-8}	2.7×10^{-6}	2.7×10^{-12}
60	1.2×10^{-5}	4.6×10^{-3}	1×10^{-4}	4.6×10^{-7}	2.45×10^{-8}	2.6×10^{-9}	3.2×10^{-8}	3.2×10^{-12}	3.2×10^{-8}	6×10^{-5}	3.84×10^{-7}		
40	1×10^{-6}	3.9×10^{-4}	3×10^{-4}	1.2×10^{-7}	6.1×10^{-8}	1.5×10^{-9}	6.2×10^{-9}	1.9×10^{-12}	6.2×10^{-9}	9×10^{-5}	1.1×10^{-7}	1.0×10^{-4}	
30	1.2×10^{-5}	4.6×10^{-3}	1×10^{-3}	4.6×10^{-6}	9.8×10^{-8}	9×10^{-8}	1.3×10^{-7}	1.3×10^{-10}	1.3×10^{-7}	1.6×10^{-4}	4.2×10^{-6}	3.2×10^{-4}	
20	4×10^{-7}	1.5×10^{-4}	5.6×10^{-3}	8.4×10^{-7}	2.45×10^{-7}	4.1×10^{-8}	9.5×10^{-9}	5.3×10^{-11}	9.5×10^{-9}	4.4×10^{-4}	8.4×10^{-7}	1.7×10^{-3}	
10	1×10^{-7}	3.9×10^{-5}	2.2×10^{-2}	8.6×10^{-7}	9.8×10^{-7}	1.6×10^{-7}	9.8×10^{-9}	2.1×10^{-10}	9.6×10^{-9}	1.6×10^{-3}	3.1×10^{-6}	2.7×10^{-2}	2.7×10^{-7}
5.7	4×10^{-8}	1.5×10^{-5}	7.9×10^{-2}	1.2×10^{-6}	4.2×10^{-6}	1×10^{-6}	1.2×10^{-8}	9.3×10^{-10}	1.1×10^{-8}	6.4×10^{-3}	1.4×10^{-5}	2.1	8.4×10^{-5}
4	2×10^{-8}	7.5×10^{-6}	1.3×1^{-1}	9.75×10^{-7}	1.12×10^{-5}	2.2×10^{-6}	1.2×10^{-8}	1.5×10^{-9}	1.05×10^{-8}	1.5×10^{-2}	3.15×10^{-5}	1	2.5×10^{-5}
2.6	1.8×10^{-8}	6.9×10^{-6}	2.5×10^{-1}	1.7×10^{-6}	1.75×10^{-4}	6.10^{-5}	2.6×10^{-8}	6.3×10^{-9}	1.9×10^{-8}	3.36×10^{-1}	1.2×10^{-3}	4	1.52×10^{-4}
1	1.5×10^{-8}	5.8×10^{-6}	5.6×10^{-1}	3.2×10^{-6}	1.4×10^{-5}	9×10^{-6}	1.5×10^{-7}	8.1×10^{-8}	6.9×10^{-8}	2×10^{-2}	2.8×10^{-4}	1.25	1.25×10^{-4}
0.5	1.3×10^{-8}	5.0×10^{-6}	7×10^{-1}	3.5×10^{-6}	1.4×10^{-5}	9.8×10^{-6}	5.1×10^{-7}	3.5×10^{-7}	1.6×10^{-7}	2×10^{-2}	6.4×10^{-4}	1.1	
0.2	1×10^{-8}	3.9×10^{-6}	7.9×10^{-1}	3.1×10^{-6}	1.4×10^{-5}	8.7×10^{-6}	2.5×10^{-6}	2×10^{-6}	5×10^{-7}	2×10^{-2}	2×10^{-3}	1.0	

PLATE 16

ANGULAR PLATFORM MOTION COMPONENTS

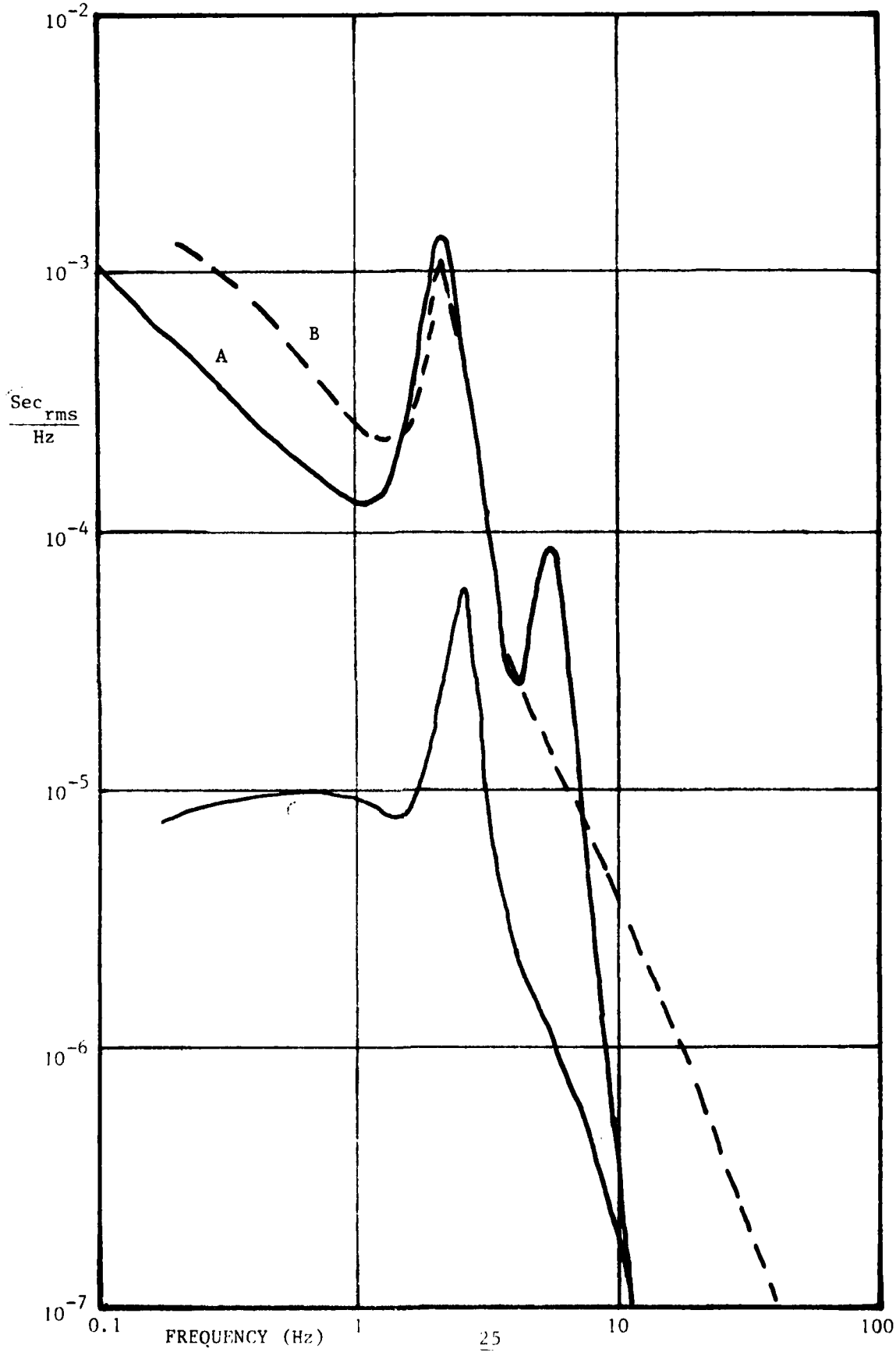

PLATE 17

bridge (displacement pick-off). They have a second pick-off coil which can be used to adjust the damping coefficient. The instruments seem to be of good quality and are surprisingly inexpensive so that the high number of instruments which provides a certain redundancy is justified.

To facilitate the understanding of how the seismometers are proposed to be used, Pl 18 gives an overview of their pertinent characteristics. Their transfer function is of second order and the exponent, x, of the numerator function depends on the input quantity of interest and on the pick-off from which the output is taken. With x defined it can be shown how the transfer function behaves at low frequencies (below the natural frequency) and at high frequencies (above the natural frequency). As an example, if linear acceleration is the input quantity of interest and the output is taken from the velocity pick-off then x = 1 and the output at low frequencies is proportional to s and at high frequencies to 1/s. It must be noted that the instrument is capable of measuring angular displacement because through such a displacement it picks up a component of the gravity vector and the resulting measured acceleration can be interpreted in terms of angular displacement.

In the proposed system scheme the seismometers measure translational motions in their respective reference planes and if more than one instrument is avaliable in each direction the redundancy is used to establish an optimum estimate. Of particular interest is the approach taken to measure angular platform motions. This is described on Pl 19. Using as an example the tilt motions about a horizontal axis, the sketch of the geometry shows that one horizontal and two vertical seismometers are used for the purpose. At low frequencies, the angular information is taken from the displacement pick-off of the horizontal instrument, which, according to the table in Pl 18 is constant in this region. Of course, the instrument is also sensitive to translational accelerations but these are negligible in this frequency range.

SEISMOMETER OVERVIEW

General Transfer Function

$$T = \frac{K \cdot S^x}{S^2 + 2\xi\omega_n S + \omega_n^2}$$

For Sprengnether Seismometers S-5100 H and S-5100 V

$$\omega_n = 0.003 \times 6.28 = 1.89 \times 10^{-2} \ \frac{\text{rad}}{\text{Sec}}$$

ξ is adjustable through separate pick-off coil

Input	Velocity pick-off $K = K_v$		Displacement pick-off $K = K_p$	
Linear acceleration	x = 1		x = 0	
	Low S	High 1/S	Low const	High $1/S^2$
Linear velocity	x = 2		x = 1	
	Low S^2	High const	Low S	High 1/S
Linear displacement	x = 3		x = 2	
	Low S^3	High S	Low S^2	High const
Angular displacement	x = 1		x = 0	
	Low S	High 1/S	Low const	High $1/S^2$

PLATE 18

ANGULAR MEASUREMENT

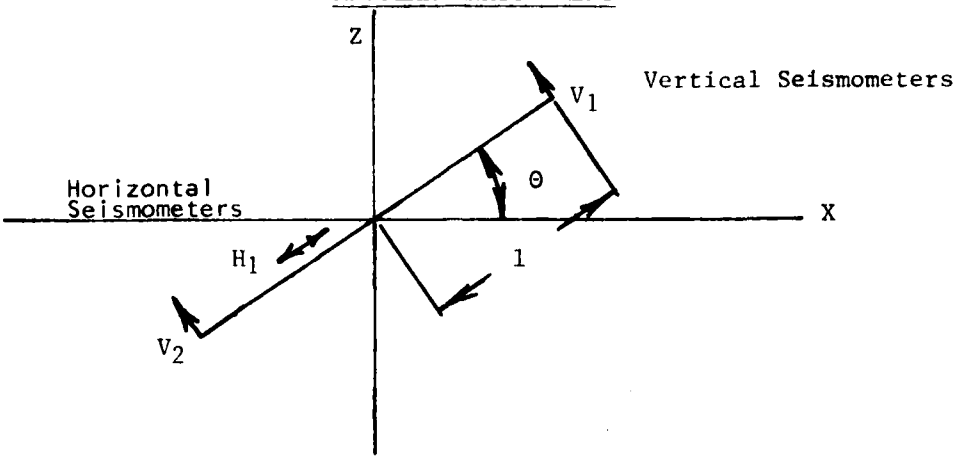

Angular information output α:

At low frequencies:

From displacement pick-off of H_1: $\alpha_L = \Theta \cdot g$: constant response

At high frequencies:

From velocity pick-off of V_1 and V_2: $\alpha_H = V_1 - V_2$

$= \dot{\Theta} l \ (k_1 + k_2)$

$= \Theta s l \ (k_1 + k_2)$

To equalize high frequency output, a filter with response $\frac{1}{1 + S/\omega_n}$ is required

PLATE 19

At high frequencies the angular information is obtained by differencing the velocity outputs of the two vertical seismometers. Each instrument measures the vertical velocity due to the tilt rate as described on Pl 19. With respect to tilt rate the output is constant in this frequency range, but if the tilt angle is defined as the quantity of interest then the output is proportional to s and a filter with an intergrating response must be used to equalize it. Then, if the scale factors of the horizontal seismometer and of the two vertical seismometers are matched a constant transmissibility at low and high frequencies is obtained. There are some deviations in the transition zone between the two frequency ranges and around the natural frequency of the instrument. This is discussed in detail on p. D-15 and it is shown that these deviations are tolerable if the damping ratio of the instruments is adjusted to 0.4-0.5.

Now, the vertical seismometers measure linear vertical velocity in addition to the velocity induced by the tilt rate. This effect is discussed in detail on Pl 20. In theory, this undesired velocity output is eliminated by differencing the two seismometers outputs. But if the scale factors of the two instruments are not exactly equal a certain undesired output remains. Based on the quantitative knowledge of the angular and linear motions of the platform, the last column of the table in Pl 20 shows the maximum admissible unbalance of the two instruments. The requirements are high but tolerable at high frequencies but increase in severity with decreasing frequency. Somewhat disturbing is the fact that very little is known about translational motions in the frequency range below 0.2 Hz. It is very well possible that the balance requirements become even more severe at frequencies below 0.2 Hz which would probably make the proposed angular measurements scheme impractical.

It is therefore absolutely necessary that an in-depth analysis of this problem area is performed before a final decision with respect to instrumentation is made. This analysis must be based on extensive

Seismometer Unbalance Effect

Actual seismometer outputs:

$V_1 = k_1 (\dot{\theta}1 + v)$

$V_2 = k_2 (-\dot{\theta}1 + v)$

$V_1 - V_2 = \dot{\theta}1 (k_1 + k_2) + v \cdot (k_1 - k_2)$

v = Vertical linear velocity

To make undesired output $v(k_1-k_2)$ equal to or smaller than desired output $\dot{\theta}1 (k_1+k_2)$

$$\frac{\Delta k}{2k} \leq \frac{\dot{\theta}1}{v}$$

On actively stabilized platform:

$\dot{\theta}_p = \dot{\theta} \cdot T_\theta$; T_θ: active transmissibility from p. D-30 $\dot{\theta}$ Derived from P1 16

$v_p = \frac{a^1 p}{\omega}$; a^1_p taken from P1 15

1=66"

f	$\dot{\theta}1$ in/Sec	T_θ	$\dot{\theta}_p \cdot 1$ in/Sec	a^1_p in/Sec^2	v_p in/Sec	$\frac{\dot{\theta}_p \cdot 1}{v_p}$
30	2.07×10^{-7}	3.2×10^{-3}	6.6×10^{-10}	4.6×10^{-6}	2.44×10^{-8}	2.7×10^{-2}
20	2.07×10^{-7}	5.2×10^{-3}	1.08×10^{-9}	8.4×10^{-7}	6.67×10^{-9}	1.6×10^{-1}
10	2.07×10^{-7}	1×10^{-2}	2.07×10^{-9}	8.6×10^{-7}	1.36×10^{-8}	1.52×10^{-1}
4	2.07×10^{-7}	1.4×10^{-2}	2.9×10^{-9}	9.75×10^{-7}	3.88×10^{-8}	7.47×10^{-2}
1	2.07×10^{-7}	2×10^{-2}	4.1×10^{-9}	3.2×10^{-6}	5.1×10^{-7}	8×10^{-3}
0.2	2.07×10^{-7}	2.8×10^{-2}	5.8×10^{-9}	3.1×10^{-6}	2.47×10^{-6}	2.35×10^{-3}

PLATE 20

in-situ measurement of angular and linear motions and on a critical evaluation of the expected stability of the instruments. The frequency range between 10^{-1} and 10^{-2} Hz is particularly problematic because it involves ground motions which are caused by the so-called microseisms which in turn are due to ocean waves pounding on the continental shelf and which are not fully understood. The discussion on page 3 of Appendix B will lead to a better understanding of this phenomenon.

3.3 Active Loop Analysis

While introducing some sound and interesting ideas such as using only one type of instruments and using a digital computer in the control loop, the presentation of the Design Analysis for the Active Control System in chapter D of subject report is rather sloppy. This is so because in many cases unit dimension information is missing or erroneous, symbols are not defined or confusing, indices are mixed up, equations are not numbered and in some cases incomplete, and the validity of some results is suspect. The major deficiency is the lack of emphasis given to the analysis of rotational (angular) motions which is particularly deplorable because these motions are the main contributor to test errors as demonstrated in par. 2 above. The analysis conducted by this author therefore will concentrate on angular motion to fill this gap.

The first task is to calculate the passive angular transmissibility function which can not be found anywhere in the report. Pl 21 presents the pertinent transfer function which is structured in accordance with the translational transmissibility function on p. D-3. This is done despite the fact that it does not agree with the equations of rotational motion on p. D-5. But these are suspect because they do not agree with the block diagram on p. D-7 which seems

PASSIVE ANGULAR TRANSFER FUNCTION

$$\frac{\Theta_2}{\Theta_D} = \frac{S^2 \cdot E(3) + S \cdot E(2) + F(1)}{S^4 \cdot F(5) + S^3 \cdot F(4) + S^2 \cdot F(3) + S \cdot F(2) + F(1)}$$

Θ_2: Angular displacement of primary reaction mass

Θ_D: Angular displacement of ground

$E(3) = B_1 \cdot B_2$

$E(2) = K_1B_2 + K_2B_1$

$F(1) = K_1K_2$

$F(2) = K_1B_2 + K_2B_1$

$F(3) = I_2K_1 + I_2K_2 + B_1B_2 + I_1K_2$

$F(4) = I_2B_1 + I_2B_2 + I_1B_2$

$F(5) = I_1I_2$

I_2: Moment of inertia of primary reaction mass: 8.13×10^3 [lb in Sec^2]

I_1: Moment of inertia of secondary reaction mass: 7.43×10^3 [lb in Sec^2]

K_2: Spring constant of upper springs: 3.42×10^6 [lb in]

K_1: Spring constant of lower springs: 5.12×10^6 [lb in]

B_2: Torque coefficient of upper springs:

B_1: Torque coefficient of lower springs: } 9.7×10^3 [lb in Sec]

NOTE: All coefficients are defined per spring and not for the whole system.

PLATE 21

to represent the physical reality quite well. Pl 21 further gives the definition of the coefficients of the transfer function for tilt motions about a horizontal axis and a quantitative list of the pertinent physical coefficients. They are derived from the coefficients which lead to the translational transmissibility function on p. C-54 by multiplying the spring related constants by d^2, where d is the distance of the spring from the center line of the platform. A list of rotational coefficients given in Table D-1 on p. D-19 is highly suspect and was not used because, besides erroneous unit dimension information, it gives different values for the inertia in the two horizontal directions which can not be explained because the platform structure is symmetrical.

Furthermore, it looks like some of the coefficients are defined for the whole system while others are on a "per-spring" basis. The top curve on Pl 22 shows the passive transmissibility function for tilt motions about a horizontal axis. It will be noted that it is quite similar to the vertical translational transfer function of p. C-54, as must be expected. In particular it shows the steep 4th-order drop-off at high frequencies, a factor which is important for the following discussions.

For the analysis of the active angular control system, Pl 23 shows first the transfer function describing the response of the platform angle to torques applied to the platform by the electromagnetic actuators. The equation is formulated in accordance with the equation for translational motions on p. D-5. The pertinent additional coefficients are defined.

The dependence of the stabilization torque on the platform angle, the missing link for loop closure, is described by the next equation. Its simple form is justified for the following reason: As explained in Pl 18 and Pl 19, the angular transmissibility of the seismometers with equalizing filter in the critical high frequency range is constant. The electromagnetic actuators are expected to have a bandwidth of 20 Hz (see p. 24), so they do not contribute

ANGULAR TRANSFER FUNCTIONS

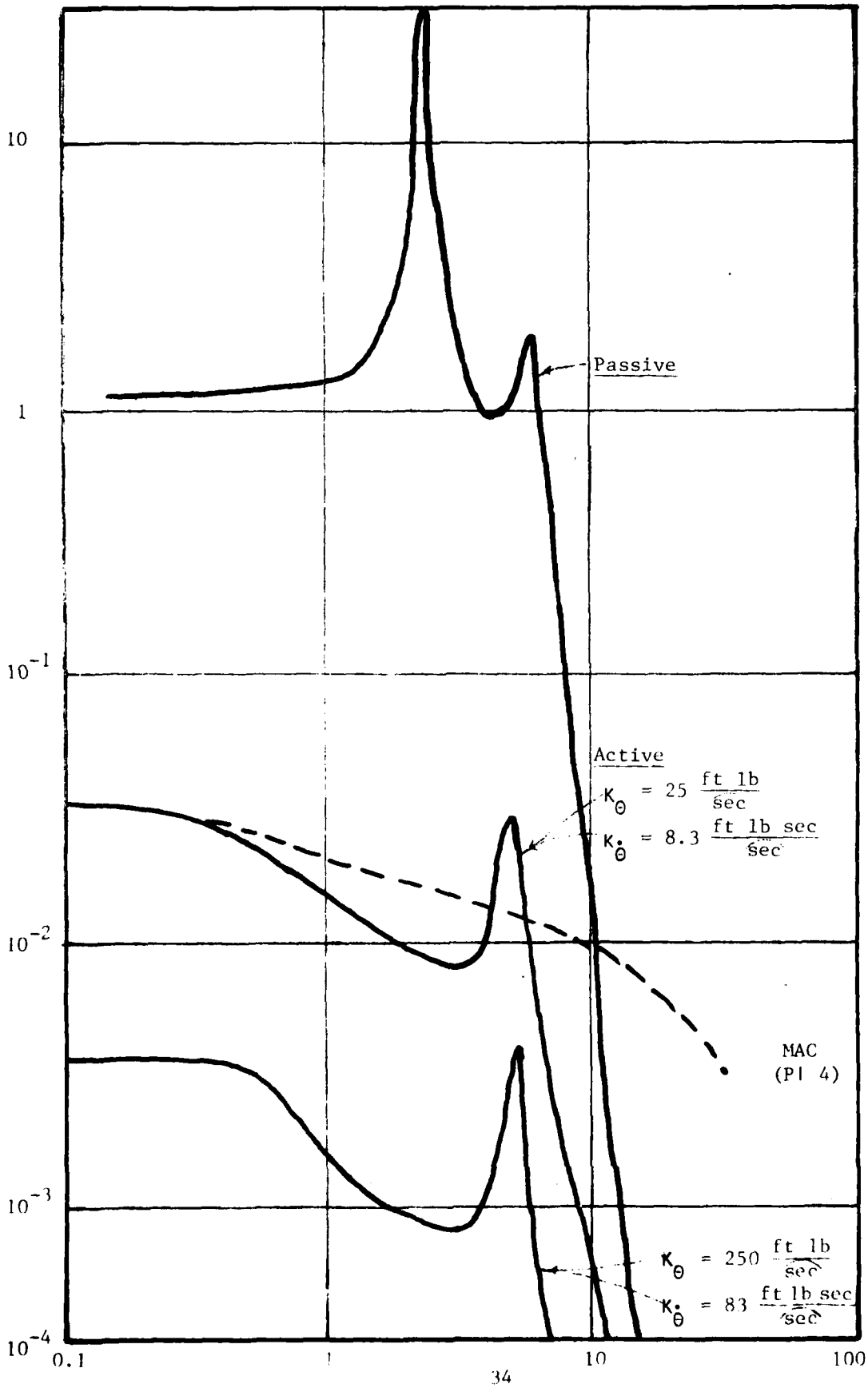

PLATE 22

ACTIVE ANGULAR CONTROL LOOP

$$\frac{\Theta_2}{T} = \frac{S^2 \cdot I_1 + S\ (B_1 + B_2) + (K_1 + K_2)}{S^4 \cdot F(5) + S^3 \cdot F(4) + S^2 \cdot F(3) + S \cdot F(2) + F(1)}$$

T: Torque applied to primary reaction mass by electromagnetic actuators. [lb in]

$$\frac{T}{\Theta_2} = K_\Theta + SK_{\dot\Theta}$$

K_Θ: Position feedback coefficient [lb in]

$K_{\dot\Theta}$: Rate feedback coefficient [lb in sec]

CLOSED LOOP TRANSFER FUNCTION

$$\Theta_2 = \frac{\Theta_D[S^2 \cdot E(3) + S \cdot E(2) + F(1)] - \Theta_2\ (K_\Theta + SK_{\dot\Theta})\ [S^2 I_1 + S\ (B_1 + B_2) + (K_1 + K_2)]}{S^4 \cdot F(5) + S^3 \cdot F(4) + S^2 \cdot F(3) + S \cdot F(2) + F(1)}$$

$\frac{\Theta_2}{\Theta_D}$: Numerator function: $S^2 \cdot E(3) + S \cdot E(2) + F(1)$

Denominator function: $S^4 \cdot F(5) + S^3 \cdot \{F(4) + K_{\dot\Theta} \cdot I_1\} + S^2 \cdot \{F(3) + K_\Theta\ I_1 + K_{\dot\Theta}\ (B_1 + B_2)\}$
$+ S \cdot \{F(2) + K_\Theta (B_1 + B_2) + K_{\dot\Theta}\ (K_1 + K_2)\} + \{F(1) + K_\Theta\ (K_1 + K_2)\}$

Θ_D: Angular Ground Motion

PLATE 23

any dynamic terms in the frequency range of interest either. Thus it is possible to describe the feedback as the sum of position and rate feedback gains. An acceleration feedback was not considered in this analysis nor were there any additional compensation terms introduced.

Finally, Pl 23 presents the complete closed loop transfer function. Thanks to the simplified form of the feedback term, the closed loop equation is manageable for evaluation by pocket calculator and two results are shown on Pl 22.

These results deserve thorough discussion. Concentrating first or the middle one it is seen that it differs significantly from the active angular transmissibility of subject report on p. D-30 which was the basis for all analyses in previous chapters of this evaluation. While the two agree well at low frequencies (the feedback coefficients were selected accordingly) there are wide discrepancies at high frequencies. In particular, the steep 4th - order drop-off is missing at the MAC function. This is important because the higher attenuation at high frequencies which contribute significantly to the test errors indicates that the active angular stabilization system actually is better than anticipated from the results of subject report. Of course, the question arises: Which of the two functions is valid? The fact that the high frequency active response coincides well with the passive response for translational motions (see Pl 2) indicates that the same must be expected for angular motions. It does not make any sense if the active response is inferior to the passive response at these frequencies, because then the active system instead of stabilizing would be destabilizing. There is no evidence that subject report uses any additional compensation terms. The only difference between the two approaches is with respect to the feedback terms. The formulas on top of p. D-18 show the feedback term used by MAC. In addition to position and rate feedback it uses

acceleration feedback and a low-pass filter with 31.8 Hz natural frequency (see Table D-2 on p. D-19). The term is somewhat suspect because it goes to 0 if there is no acceleration feedback. In any case, use of this feedback term can not explain the slow drop-off at high frequencies. It must then be concluded that our transfer function, though based on certain simplifications, is valid while the MAC function is not, because its character can not be explained with the information available at this point.

It is of importance to point out that the loop is stable under the feedback conditions selected. This suggests to try an even tighter feedback. The lower curve on Pl 2 shows one result. Its general attenuation level is about one order of magnitude higher than before and the loop is still stable. However, there is indication that the stability limit is being approached because the resonance peak at 5.2 Hz is more pronounced. There was no time to determine the stability margins by open loop analysis.

In conclusion, it can be stated that there is strong evidence that the active angular control system is better than expected by the contractor's analysis. This is due to the fact that there is significantly higher attenuation at high frequencies and that the feedback loop can be tightened without endangering stability. The potential improvement is estimated at one to one and a half order of magnitude which would make it possible to reach the test goals spelled out on Pl 8 and Pl 10. However, caution is indicated because simplifications were used in the present analysis and an in-depth computer analysis is required.

4. Conclusions and Recommendations:

1. The passive isolation system is basically sound and in combination with the active system, as described in subject report, is

compatible with the state of the art. However, there is strong evidence that the active stabilization loop actually is better and can be even more improved. In this way it seems possible to eventually provide a capability to test gyros with a drift rate of 10^{-6} $(deg/hr)_{rms}$ and accelerometers with a noise level of $10^{-8} g_{rms}$.

2. There is a certain crosscoupling between translational and rotational motions due to the excitation of rocking motions. At the given disturbance input levels, these rocking motions are of the same order of magnitude as the natural rotational motions and as such are not dangerous. However, the analysis performed used certain simplifications and it is necessary to perform an in-depth computer analysis when the final system constants are known and more information on the disturbance inputs at the test site will be available.

3. A similar crosscoupling between translational and rotational motions is due to the gain unbalance of the two seismometers which measure angular motions. The present analysis indicates that the relative difference of the gain factors must not exceed a few parts in 10^{-4} to avoid that the induced angular motion is larger than the natural angular motion. This is already a requirement on the border line of realizability. It is therefore necessary that an in-depth analysis be performed, based on the most reliable measurements of the input disturbances at the test site and a critical review of instrument stability, before a final decision is made on the scheme of using two balanced seismometers for measuring angular motions.

4. From the foregoing analysis it is evident how important the knowledge of actual angular and translational motions at the test site is. In particular, it is necessary to provide more information at least down to frequencies of about 10^{-2} Hz to cover the range of the so-called microseisms. The interaction of translational and rotational motions in this range depend heavily on the test site. It is therefore necessary to perform an extended series of measurements at the test site, using instrumentation which clearly distinguishes between rotational and translational motions.

5. While not directly a part of this evaluation, it is suggested that the analysts of future tests performed on the platform develop a deep understanding of the platform characteristics. This will enable them to recognize events which are caused by the platform and not by the test item and to eliminate them from test data. Examples are rocking motions of the platform. Related to this are events like airplane overflights or sled runs the time of occurence of which can easily be identified and their effects on the test data, if any, can be eliminated.

6. A further improvement of test accuracy can be achieved if the test analyst critically determines what frequency ranges are of actual interest to the item under test. As an example, a gyro under test may not have a quick reaction requirement and consequently corresponding higher frequencies can be filtered out from the test data. This can lead to a substantial reduction of noise level.

Appendix A

Discussion of Data Presentation Format

The variables we have to deal with, rotational and translational ground motions and their derived quantities, are random

processes. The frequency components of such processes do not have defined phase relationship and thus the only possible way of their spectral representation is by the Power Spectral Density Functions (PSD) or Power Spectra, which have a dimension of $\widehat{sec}^2/Hz$, using a rotational quantity as an example. For a detailed discussion of this see Ref. 6. These power spectra make it possible to determine the over-all rms value of the variable in a given frequency band by integrating the power spectrum over this frequency band. In this way the total "power" in the band is obtained and by taking the square root the rms value. In the Second Design Review Meeting of 8 Mar 80, it was agreed to use a "rms spectrum" or "amplitude spectrum" for the presentation of the data, in our example having a dimension of $\widehat{sec}$rms/Hz. This can be obtained by taking the square root of the power spectrum at each frequency. This is perfectly legal and physically meaningful. Instead of saying: my variable has so much "power" in a frequency interval of 1 Hz it is stated now that it has such and such rms value in this interval of 1 Hz.

However, there is a possible trap: It is not possible to determine the over-all rms value of a variable by integrating the rms spectrum over frequency. To determine the overall rms value it is necessary first to obtain the power spectrum by squaring the rms spectrum point for point, then integrating the power spectrum over frequency to obtain total power and finally by taking the square root obtainning the over-all rms value.

Appendix B

See attached paper titled, A Proposed Model for the Rotational Motions of a Test Pad.

List of References

1. W. J. Whitesell and Major T. R. Hooten: "Program and Plans for the Development of a Presision Guidance Test Facility." Paper presented at the Ninth Guidance Test Symposium, Holloman AFB, Oct 79. ADTC-TR-79-11 (AD A076-567).

2. Bill J. Simmons, Frank J. Seiler Research Laboratory, USAF Academy, Colorado: "A Sub-Seismic Test Platform as Motion Exciter." 1979 Proceedings of the Instrument Society of America ISBN 8764-434-5 pp. 167-178.

3. Emil Broderson, F. J. S. Research Laboratory: "Stabilization of a Seismic Isolation Block Instrument Testing", AIAA Paper No. 74-857, Aug 74.

4. Herbert Weinstock, NASA Electronics Center, Cambridge, MA: "Design of a Precision Tilt and Rotational Vibration Isolation System for Inertial Sensor Testing", AIAA Paper 68-894, Aug 68.

5. Martin G. Jaenke, AFMDC, Holloman AFB: "The Dynamic Characteristics of Test Pads", AIAA Paper 69-860, Aug 69.

6. William D. Koenigsberg: "Spectral Analysis of Random Signals-Techniques and Interpretations", CSDL Report E-2771, Jun 73.

7. Measurement Analysis Corporation: "Design and Analysis of a Seismically Stable Platform", MAC Technical Report TR-7015.003, Jun 80.

Sponsored by—
American Institute of Aeronautics and Astronautics (AIAA)
With Participation of—
American Astronautical Society (AAS)

AIAA Paper No. 74-855

A PROPOSED MODEL FOR THE ROTATIONAL MOTIONS OF A TEST PAD

by
MARTIN G. JAENKE
U.S. Air Force Central Inertial Guidance Test Facility
Holloman Air Force Base, New Mexico

AIAA Mechanics and Control of Flight Conference

ANAHEIM, CALIFORNIA / AUGUST 5-9, 1974

A PROPOSED MODEL FOR THE ROTATIONAL MOTIONS OF A TEST PAD

Martin G. Jaenke*
Technical Advisor
Central Inertial Guidance Test Facility
The CIGTF of the US Air Force
AFSWC, 6585th Test Group/GD
Holloman AFB, NM 88330

Abstract

Based on pad motion measurements at various test sites, the model is formulated as the power spectral density function of angular deflections. Basically, it consists of a random walk process which is well defined over 10 decades of frequency. Superimposed are two peak areas, one of them reflecting diurnal fluctuations and the other motions due to microseisms. The properties of these processes and their estimated tolerances are discussed. However, the mechanism of the fluctuations due to microseisms is not yet fully understood and additional experimental and theoretical work is solicited. Derived from the model are the expected uncertainty in the orientation of an azimuth reference monument as a function of time after calibration and the angular rates which will be sensed by a gyro under test.

I. Introduction

The ever increasing accuracy of gyroscopes makes the testing of these instruments without undue interference by external perturbations increasingly difficult. One source of perturbations which is of particular significance is the rotational motion of the pad on which the gyro is tested, a motion which is represented by its three components: North-South (NS) tilts, East-West (EW) tilts, and changes in azimuth orientation. The concern with this motion environment is certainly not new. Extensive measurements of the motion components have been made by many test agencies and various approaches to obtain control over these motions are under way. However, what is missing at this time is a quantitative understanding of the functional character of this motion environment. Availability of such an understanding, in other words the existence of a "model" would facilitate the optimization of test procedures in the following areas: Calibration of the azimuth orientation of a test pad, compensation of tilt and azimuth motions and optimum filtering of the gyro outputs during a test.

It is therefore, the purpose of this paper to review and compile data which were taken at representative test sites with the goal of comparing magnitudes and detecting common trends. As a result, a quantitative model will be formulated and its uncertainties will be discussed. Thus the modeling process is purely empirical and inductive, concentrating on the phenomena which are of practical interest to the test engineer and attempts of a physical explanation of the model will be very limited. However, the surprising agreement with a theoretical model which was derived deductively many years ago will be noted and the ensuing possibilities for a physical explanation of the observed phenomena will be discussed. Finally, basic considerations concerning the application of the proposed model will be presented.

The ultimate purpose of the paper is an appeal to the Geokinetic Community to create a data pool which is much more comprehensive than the one which is presently available. This then will allow formulating a model with much higher confidence than is presently possible.

II. Compilation of Data and Formulation of the Model

An overview of available rotational motion data indicates that deterministic trends are either non-existent or very weak. The analytical tool for describing such data thus has to be of statistical nature and for the purposes of this paper the tools of time-series analysis will be used. In particular power spectral density functions, in short, power spectra, will be used to describe the measured data. This then allows using the related descriptors, namely, cross-correlation spectra, transfer functions and coherence functions as powerful tools for further investigations. Power spectral analysis is not new but has come into widespread use only fairly recently after the full development of the Fast Fourier Transform and the availability of minicomputers made the on-line and near real-time computation of power spectra a practical possibility. Reference 1 describes this analytical method in detail and discusses its limitations.

The frequency range of a power spectrum describing the angular motions which are of interest for gyro testing is extremely wide, extending from about 100 Hz to 10^{-8} Hz, a span of 10 orders of magnitude. The upper limit is due to the necessity of determining gyro noise within the pass-band of a platform stabilization loop, the lower one is connected with the interest in the behavior of azimuth reference monuments and in the long-term stability measurements of gyros. As will be shown, it is possible to formulate a model in terms of an angular deflection power spectrum which is meaningful over this wide frequency range. The quantity of interest, angular deflection power density, covers a span of 20 orders of magnitude. Quite certainly a phenomenon extending over such an extremely wide range of magnitudes cannot be observed by a single type of instrument or one single method. It is rather necessary to perform measurements within restricted frequency bands using instruments and methods which are suitable for the respective range.

Representative results of measurements made in various frequency ranges are presented in the following figures. The data used are extracted and transcribed from the sources which are identified in the figures. To make the compilation of many data in one figure possible and still avoid overcrowding, the connecting lines between data points are omitted. Furthermore, only such data points were transferred from the original source which are required to reflect realistically the trends and uncertainties of a given spectrum.

* Associate Fellow AIAA

Figure 1 covers the two decades from 1 Hz to 100 Hz. The measurements are made with arrays of seismometers. In this way it is possible to measure all three components of angular motion, NS tilt, EW tilt, and fluctuations in azimuth. An important phenomenon in this frequency range are spikes which are clearly due to cultural activities, such as the spikes at 60 Hz and near 30 Hz. Figure 2 shows the two tilt components in the range from 10^{-4} Hz to 1 Hz. The measurements are made with tilt meters, azimuth information is not available in this range. Of particular interest is a peak centered at about 0.15 Hz. It is due to microseismic activities and will be discussed in detail later. Figure 3 covers the range from about 10^{-6} Hz to 10^{-2} Hz. Again, the measurements are made with tiltmeters and azimuth information is not available.

Finally, Figure 4 presents azimuth data in the range from about 10^{-8} Hz to 10^{-6} Hz. Tilt information in this range is not available. The data are derived from the calibration of the azimuth orientation of reference monuments with respect to Polaris. This type of data is usually not very well suited for power spectral analysis because the observations are normally unequally spaced in time. However, the spectrum shown was derived from a set of measurements which were fairly regularly spaced at intervals of two months, and thus it can be considered meaningful. But even if only irregularly spaced data are available, it is still possible to make a reasonable low-resolution estimate of power density. Assume that n measurements are available, irregularly spaced over an observation interval T. Then the variance of the measurements can be calculated after extraction of the mean and linear trend from the data. This variance is the total power in the frequency band between 1/T Hz and n/2T Hz and a mean power density in the theoretical frequency band of width 1/T (n/2 - 1) Hz can be calculated. Some results of this type are shown in Figure 4. This method admittedly is crude and has its shortcomings, in particular with respect to the definition of the upper frequency limit. However, it is considered adequate for an order-of-magnitude check of spectral density of a given series of irregularly spaced observations.

To obtain a comprehensive overview of the character of the rotational motion under study, the information from Figures 1 - 4 is compiled in Figure 5. Again, only such data are transferred which are necessary and sufficient to provide adequate trend and dispersion information. A first inspection of the figure shows that the individual spectra follow quite closely a $1/f^2$ law, represented by line A, over the wide frequency range from 10^{-8} Hz to 10^2 Hz. Considering that the data used are derived from three different motion components and from measurements made at different locations at different times, the dispersion about this line is quite reasonable. This line describes the underlying statistical process of the proposed model and is defined by the following equation:

$$\phi = \phi_o \left(\frac{f_o}{f} \right)^2 \qquad (1)$$

ϕ : Spectral density of angular displacement

$\phi_o = 10^8 \ \frac{\widetilde{(sec)}^2}{Hz}$ with an uncertainty range from 10^7 to $10^9 \ \frac{\widetilde{sec}^2}{Hz}$

$f_o = 10^{-8}$ Hz

The uncertainty of ±1 order of magnitude may seem large but is considered reasonable for a phenomenon whose magnitude range of interest extends over 20 decades.

The underlying statistical process then i random walk. There is some evidence that this process is actually an "exponentially correlated process", the spectral density of which would remain constant below a certain breakpoint frequency. But the available experimental data are too scarce to make a reliable quantitative estimate of such a breakpoint frequency, or, in other words, of the correlation time of the process. The data compiled in Figure 5 indicate that for observation periods up to one year, or frequencies down to 10^{-8} Hz, the assumption of a random walk is a valid representation of the underlying statistical process of the proposed model. It should be noted that the assumption of a random walk character for the angular displacements leads to a "white" character for the angular rates, a result which is intuitively appealing.

The derivation of this basic model implies that within the given tolerances, its three components are equal and that it is independent of the time and place of the observation. A review of existing literature reveals strong indications that these assumptions are reasonable. Line B in Figure 5 describes a model predicted by Weinstock[2] under the assumption that the rotational phenomenon is due to a vertical displacement wave propagating in an elastic half-space with a propagation velocity of about two miles/second. In accordance with the reference the rotational displacement spectrum is then given as:

$$\phi \left[\frac{\widetilde{sec}^2}{Hz} \right] = \frac{1.44 \times 10^6}{f^2} \cdot \phi_a \left[\frac{g^2}{Hz} \right] \qquad (2)$$

ϕ_a : Spectral density of translational vertical acceleration

In the frequency range from 10^{-5} Hz to 10^{-2} Hz Weinstock assumes constant "white" vertical acceleration power density and his prediction agrees surprisingly well with the proposed model not only trendwise but also magnitudewise. That the assumption of a white character of the translational acceleration spectrum is reasonable is confirmed by quite recent measurements published in Reference 3. The portions of these measurements pertinent to the present discussion cover the frequency range from 6.6×10^{-3} Hz to 3.3×10^{-2} Hz. In addition to confirming the character of the spectrum in this frequency range, the measurements indicate that the spectral magnitudes of the three motion components are equal to within ±20%. (Figure 9 of Reference 3); that the observed magnitudes are equal within ±25% independent of the time of the observation (Figure 10 of Reference 3) and that they are equal within ±20% independent of the place of observation. (Figure 12 of Reference 3).

Superimposed to the underlying random walk mechanism which is described above are several peak areas. The one which turns out to be most important is the one which centers at the frequency of 1.15 x 10^{-5} Hz, the period of which is one day. The strong influence of the diurnal cycle is well known and commonly observed. However, it is also known that the resulting angular motions are not deterministic and not clearly correlated to external influences, such as temperature. Apparently, the combination of physical phenomena which affect the angular motions of the diurnal cycle do not fluctuate periodically but in a random fashion. The modeling concept which seems to explain the observations quite realistically is that of a sinusoidal carrier frequency, the basic diurnal rhythm, which is amplitude modulated by random events. The spectrum resulting from such a process can be described by the following equation:

$$\phi_D = \phi_{D_o} \frac{1}{1 + \left[\frac{f - f_D}{B}\right]^n} \qquad (3)$$

ϕ_D : Spectral density of resulting angular displacements.
ϕ_{D_o} : Spectral density at 1.15 x 10^{-5} Hz, the carrier frequency.
f_D = 1.15 x 10^{-5} Hz
B : Bandwidth of the modulating random fluctuations (Hz).
n : Empirical exponent.

A review of the available data indicates that they can be represented most adequately if one assumes $B = f_D$ and $n = 4$. Physically this means that the spectrum of the modulating random forces contains primarily frequencies with periods longer than one day and falls off sharply at higher frequencies. The resulting spectrum shown in Figure 5 is calculated under the assumptions that ϕ_{D_o} is 100 times larger than the spectral density of the random walk at this frequency, that $f_D/B = 1$, and that $n = 4$.

Another significant peak in the composite spectrum is centered close to 10^{-1} Hz and is known to be due to microseisms generated by ocean waves. It is observed all over the continent if the angular measurements are made with tiltmeters. However, it has not been observed with gyros or with other instruments which sense angular motions only and are not sensitive to translational accelerations like tiltmeters. An example of a nongyroscopic instrument of this type is the fused silica angular motion sensor described by S. Okubo in Reference 4. This phenomenon of apparent nonobservability of the microseisms with instruments which are sensitive to rotational motions only seems to contradict the expectation of coupling between translational and rotational motions which was described in equation (2). However, Reference 3 points out that the earth noise within the microseismic peak is of oceanic origin but in the adjoining lower frequency range, the range which the proposed model describes as a random walk, it is of atmospheric origin. That the propagation characteristics of the noise differ substantially between the two ranges is shown in curve A of Figure 6. This curve is transcribed from Figure 4 of Reference 3, it shows the squared coherency function of two simultaneous vertical translational displacement measurements made with two seismometers placed at a distance of 153 m approximately 543 m below the local surface. While the coherence is quite strong in the microseismic peak range, it falls off sharply and significantly toward lower frequencies. Another indication of the difference of the microseismic mechanism from the one in adjoining frequency ranges is given by curve B in Figure 6. It is transcribed from Figure 3 of Reference 10 and shows an example of power attenuation of the noise with depth below the surface. While the attenuation within the microseismic peak range is small, it increases significantly at the transition to higher frequencies. Thus, with the experimental evidence presently available, it must be concluded that the spectral peak about 0.1 Hz is not truly a component of the rotational motion environment and thus it will not be included in the presently proposed model.

Other spectral peaks due to natural causes which one has to expect are located at the frequency the period of which is one year, and another one with a period of a half day. Due to the extremely long periods of observation required to describe the annual peak, very little experimental material is presently available. There is some evidence of such a peak in Figure 4, but the uncertainties of this one spectrum are too high to allow a serious modeling effort. The half-day peak is occasionally observable but is normally submerged in the envelope of the diurnal peak.

At the high-frequency end of the spectrum very high and narrow spectral peaks can be observed. (See Figure 1) As stated before, they are due to human activities and can be easily identified as such. In view of their strong dependence on local conditions they are not included in the present modeling effort.

The proposed model then is a power spectrum of rotational deflections consisting of an underlying random walk process which is observable over ten decades of frequency, superimposed to which is the spectrum of diurnal random fluctuations as described in equation (3).

III. Limitations and Uncertainties of the Model

The technique of power spectral representation of time series has certain limitations which must be kept in mind in interpreting the data. First, it is valid only for stationary series, the statistics of which do not change with time. Thus, care must be taken to avoid drawing conclusions from data which were measured during periods when unusual disturbances such as earthquakes or similar events take place. However, practical experience indicates that periods with evidently stationary characteristics prevail at test sites so that a meaningful analysis can be conducted with reasonable care. Furthermore, it must be recalled that power spectral densities computed from a finite amount of data are only estimates of the true values. The uncertainty of these estimates can be as high as ±100% if only one set of measurements is available. A detailed analysis of these uncertainties is given in Reference 1. In general, the uncertainty in a calculated spectrum increases with decreasing frequency which may lead to an erroneous determination of the slope of the spectrum. The technique applied in this paper, namely, to line up spectra measured in different frequency intervals with different instrumentation tends to de-emphasize the slope uncertainties in the individual spectra and to

provide information on the wide-range slope trends of the phenomenon under study.

In addition to the statistical uncertainties discussed above, the inherent uncertainties of the measurements must be taken into consideration. At the low end of the spectrum, the uncertainties connected with the azimuth calibration of a reference monument from Polaris observations play an important role. While the internal random noise of most tiltmeters is sufficiently low for the purposes discussed here, many of them show a significant temperature sensitivity and extreme care must be taken to avoid erroneous results due to this error source.

The claim of the proposed model to be valid within the stated tolerance limits for representative test sites seems to be contradicted by a measurement recently made at the Agassiz test station in Harvard, MA by the C. S. Draper Laboratory. The power spectrum of these measurements which was made available to the author through private communication by Mr. Koenigberg, shows values which are nearly three orders of magnitude smaller than expected from the model in the frequency range from 3×10^{-3} Hz to 3×10^{-2} Hz. This is the only significant deviation from the proposed model which is presently known to the author. However, the uncertainties of the spectrum are particularly large in this frequency range as will be noted by inspection of Figure 5. This is the transition range where motions generated by quite different mechanisms overlap and thus such large uncertainties may be explainable.

IV. Applications of the Model

The availability of such a quantitative analytical model is a valuable tool for the planning and evaluation of gyro tests in many respects. One important application is that it provides an understanding of the growth of the uncertainty in the knowledge of the orientation of an azimuth reference monument as a function of time after calibration. This information can be derived from an integration of the power spectrum over the frequency interval from $+\infty$ to $1/T$ where T is the time passed since the last calibration. This translation between the frequency and the time domain is based on the property of the Fourier transform that the lowest frequency which is theoretically defined in an observation interval T is $1/T$. Curve A in Figure 7 shows the uncertainty variance of the random walk component which increases proportional to time. Curve B is the variance connected with the diurnal peak of the model which dominates the uncertainty growth process within the time interval of practical interest. The sharp increase of the uncertainty in the time interval up to one day must be noted. The understanding of the statistical nature of the monument motions provided by the model together with the knowledge of the uncertainties of Polaris observations can be used to optimize the calibration process of the monument.

Another important application of the model is its suitability to predict the output of a gyro under test which is due to test pad motions. Curve A in Figure 8 shows the resulting power spectrum of the earth rate components which the gyro "picks up" due to its deflections from a neutral test orientation. Curve B shows the power spectrum of the pad motion angular rates which the input axis of the gyro senses. Curve C is the spectrum of the drift rates due to the pad motion angular accelerations sensed by the output axis of a representative gyro. This externally induced gyro output noise spectrum must be separated from the internal gyro noise, the quantity of interest to be determined in the test. Independent on how this separation of the noise sources is approached, either servo stabilization of the test platform or compensation in the data evaluation, the availability of a quantitative estimate of the external noise statistics is an important tool in the optimization of the respective process.

Furthermore, the knowledge of this external noise spectrum can be used to assess the deterioration of other tests due to the motions of the test pad. In Reference 5 this is done for a standard-torque-to-balance test. Studies concerning the effects on a four-position gyro compass process are under way.

V. Conclusions

The paper demonstrates that the attempt to formulate a model of angular test pad motions of general validity is not unreasonable. However, more observations are required to obtain better estimates of the tolerances of the model and its structural details. In particular, more information is needed to explore the nature of the microseism peak of the spectrum. To accomplish this it is proposed that relevant data which are either available now at various test organizations or which will be collected in the future be made available to the Geokinetics Sub-Committee of the AIAA Technical Committee on Guidance and Control. In this way a basis could be established for the preparation of a Summary Paper or a Progress Volume and the formulation of a generally recognized model.

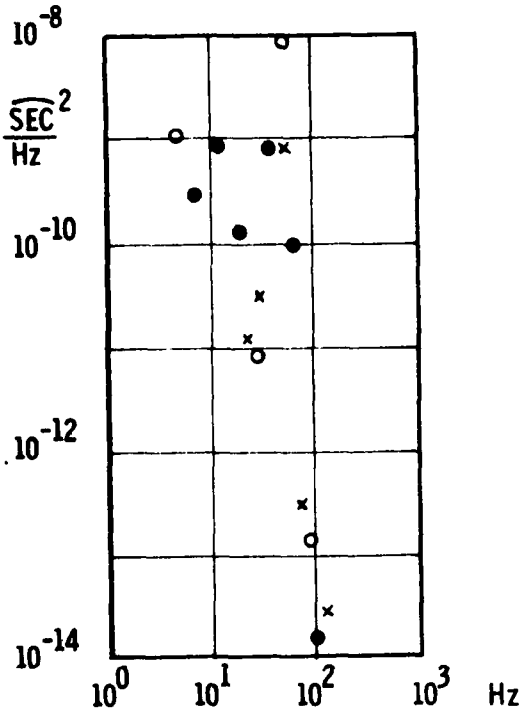

FIG. 1 SPECTRA FROM 1 - 100 Hz

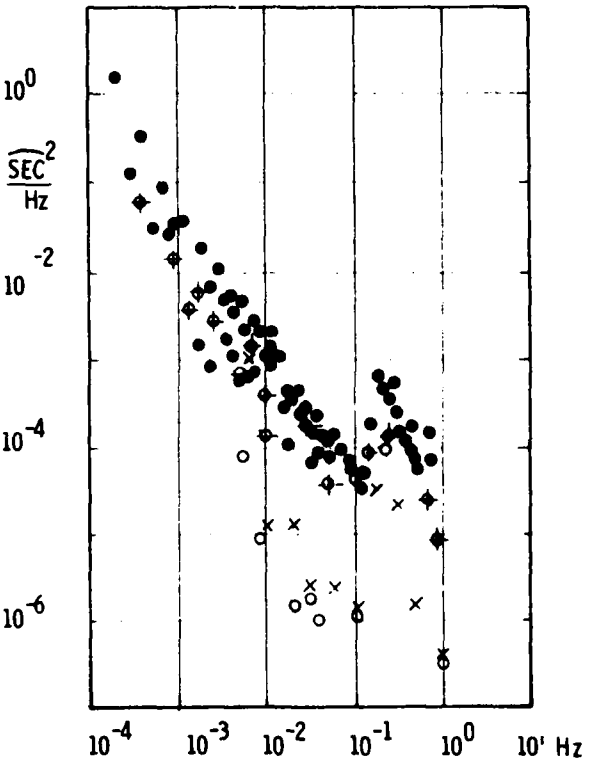

FIG. 2 SPECTRA FROM 10^{-4} - 1 Hz

● EW Tilt

○ NS Tilt

× Azimuth Fluctuations

Holloman AFB; CIL Bldg.; August 71

Pairs of Geotech Model 18300 Seismometers

● EW Tilt — Bedford Flight Fac., CSDL; Apr 73

Hughes TM 3 Tiltmeter (Reference 6)

○ EW Tilt, × NS Tilt — Holloman AFB, CIL Bldg., August 71

Geotech Model 18279 Tiltmeters

⊠ EW Tilt — Holloman AFB, CIL Bldg. April 74

ADL Mod III Tiltmeter

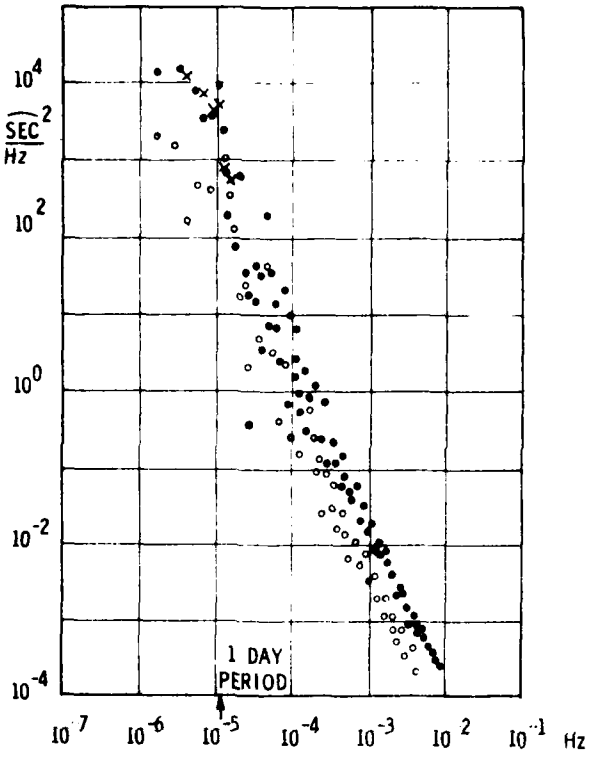

FIG. 3 SPECTRA FROM 10^{-6} - 10^{-2} Hz

● EW Tilt } Bedford Flight Fac., CSDL;
Feb - Apr 73

○ NS Tilt } Hughes TM 3 Tiltmeter
(Reference 6)

✕ Composite EW - NS Tilt Vector

Holloman AFB, Lab Bldg.,
June 67

Geotech Model 18279 Tiltmeter
(Reference 7)

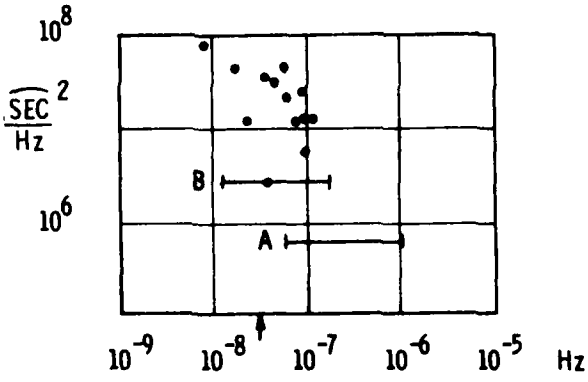

FIG. 4 SPECTRA FROM 10^{-8} - 10^{-6} Hz

● Azimuth Fluctuations. Holloman AFB;
Lab Reference Monument Calibration
Feb 70 - Dec 73 (Reference 8)

⊢—⊣ Average Azimuth Fluctuations

Anaheim, California
Autonetics R & D Azimuth Reference
Calibrations. (Reference 9)

A May - Nov 67

B Dec 67 - Feb 70

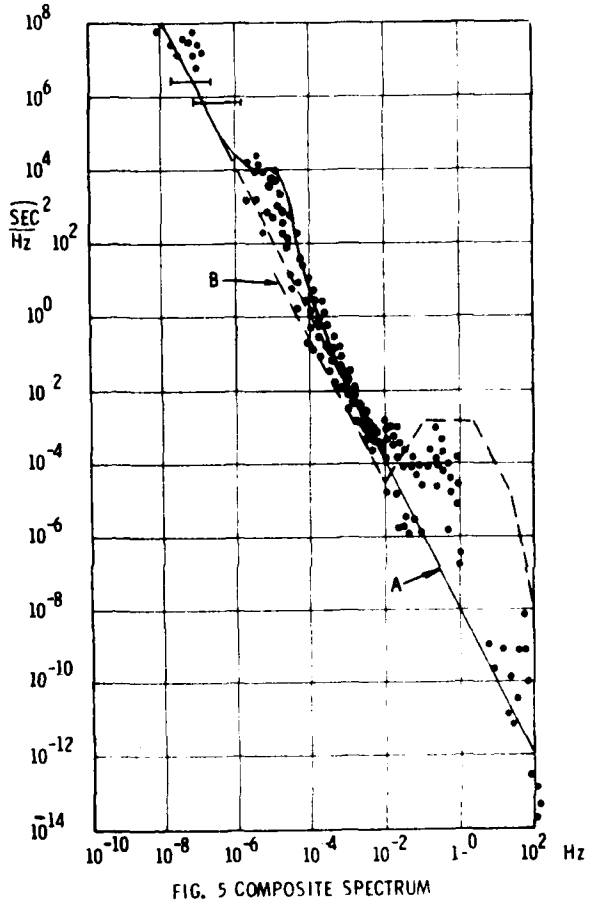

FIG. 5 COMPOSITE SPECTRUM

A : Random Walk Process

B : Weinstock's Model

(Reference 2)

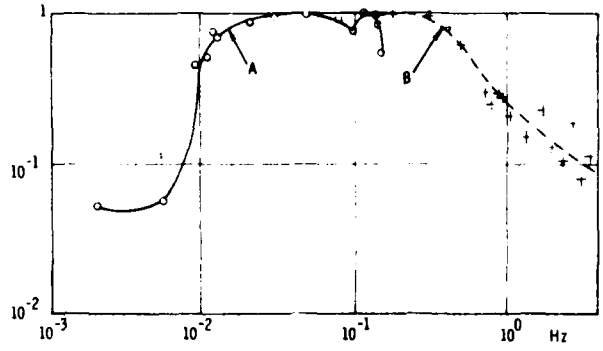

FIG. 6 PROPERTIES OF THE MICROSEISMIC PEAK

A : Squared Coherence Function of Measurements from Two Seismometers Placed at a Distance of 153 m.

(Transcribed from Reference 3, Figure 4)

B : Ratio of Power Spectral Densities of Translational Acceleration Measured at a Depth of 668 m and on the Surface.

(Transcribed from Reference 10, Figure 3)

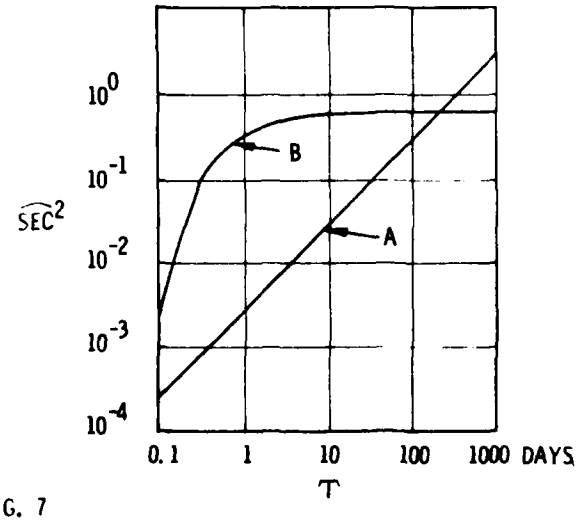

FIG. 7
GROWTH OF PAD ORIENTATION UNCERTAINTY WITH TIME

A : Influence of Random Walk Process

B . Influence of Diurnal Fluctuations

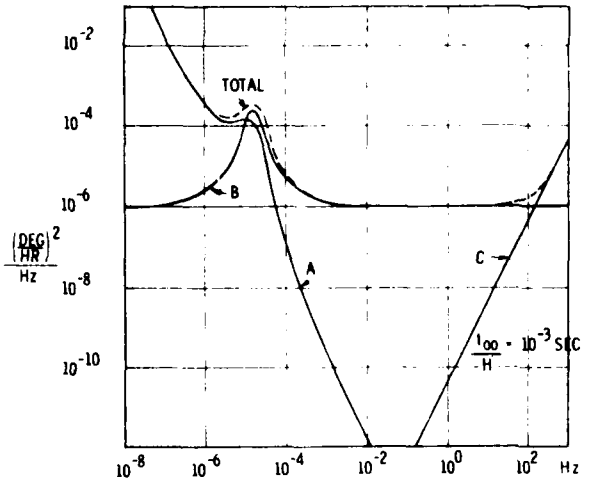

FIG. 8 PAD MOTION INDUCED GYRO NOISE

A : *Earth Rate Component*

B : Angular Rates About Input Axis

C : Angular Accelerations About Output Axis

List of References

1. William D. Koenigsberg: Spectral Analysis of Random Signals - Techniques and Interpretations, CSDL Report E-2771, June 1973.

2. Herbert Weinstock: Limitations on Inertial Sensor Testing Produced by Test Platform Vibrations, NASA TND 3683, November 1966.

3. J. Savino, K. McCamy, G. Hade: Structures in Earth Noise Beyond Twenty Seconds - A Window for Earthquakes, AFCRL-72-0358, May 72 (Bulletin of the Seismological Society of America. Vol. 62; No. 1; pp 141-176; Feb 72)

4. S. Okubo: Seismic Angular Motion Sensor; AIAA Paper No. 73-829, August 1973.

5. Judith Koestler: Investigations of the Errors Induced by Seismic Motions During Tumble Tests; Sixth Guidance Test Symposium Proceedings; AFSWC TR 72-34, October 1972.

6. William D. Koenigsberg: Evaluation of Hughes Research TM-3 Tiltmeters; CSDL Report SOSS-TST-73339, December 1973.

7. R. Blandford, F. Ruskey, V. R. McLamore: Seismic Isolations Study of the Central Inertial Guidance Test Facility; MDC-TR-68-043, May 1968.

8. Internal correspondence from Defense Mapping Agency (Geodetic Survey Squadron) to 6585th Test Group, Holloman AFB: "December 1973 Increment - CIGTF Azimuth Data Base, Project DMAAC 74-2", 21 December 1973.

9. N. W. Cherry: Establishing High-Accuracy Indoor Azimuth References; AIAA Paper No. 73-842, August 1973.

10. E. J. Douze, J. D. Kerr: The Acceleration Environment Obtainable in Deep Holes; Proceedings of the AIAA/ION Guidance and Control Conference. August 1965; pp 360-365.

DISTRIBUTION LIST

	Copies
Defense Documentation Center Cameron Station Alexandria, VA 22314	12
6585th Test Group Holloman AFB, NM 88330	10